Effect of Gravity Waves on Kelvin-Helmholtz Instability of a Shallow-Water Flow

レイ, チイタイ

https://doi.org/10.15017/2534380

Ph.D. Thesis

Effect of Gravity Waves on Kelvin-Helmholtz Instability of a Shallow-Water Flow

Thi Thai Le
Supervisor: Prof. Yasuhide Fukumoto

Graduate School of Mathematics
Kyushu University

Declaration

I, Thi Thai Le, declare that this thesis titled, "Effect of Gravity Waves on Kelvin-Helmholtz Instability of a Shallow-Water Flow" and the work presented in it are my own. I confirm that:

- This work was done wholly or mainly while in candidature for a research degree at this University.
- Where any part of this thesis has previously been submitted for a degree or any other qualification at this University or any other institution, this has been clearly stated.
- Where I have consulted the published work of others, this is always clearly attributed.
- Where I have quoted from the work of others, the source is always given. With the exception of such quotations, this thesis is entirely my own work.
- I have acknowledged all main sources of help.
- Where the thesis is based on work done by myself jointly with others, I have made clear exactly what was done by others and what I have contributed myself.

Signed:

Date:

Acknowledgements

This document would not have been possible without the support of several individuals and organizations. The following list is not complete and I would like to extend an apology to anyone who is omitted from it.

Firstly, I am very grateful to the Ministry of Education, Culture, Sports, Science and Technology, Japan for supporting me during with scholarship award during my research progress at Graduate School of Mathematics, Kyushu University, Japan.

I would like to express my sincere gratitude to my supervisor Prof. Yasuhide Fukumoto for the continuous support of my Ph.D study and related research, for his patience, motivation, and immense knowledge. His guidance helped me in all the time of research and writing of this thesis. I could not have imagined having a better advisor and mentor for my Ph.D study.

My sincere thanks also goes to Dr. Ikeda Hirosaka , Prof. Kawasaki, Prof. Shirai Tomoyuki who supported me in applying an long internship course of Doctoral Functional Mathematics Program.

I would like to thank to the staffs of Mathematics Department and Student Office of Faculty of Science for constantly supporting me whenever I asked.

I thank my fellow labmates for the stimulating discussions in research and for all the fun we have had in the last four years. Especially, I would like to thank to my Japanese labmates for supporting me in my living in Japan. Also I thank my Vietnamese friends and all of my friends in Kyushu University and in Vietnam for cheering me up during my research progress. In particular, I am grateful to Associate Prof. Trinh Khanh Duy for enlightening me the first glance of doing research aboard, especially in Japan during 4 years.

I would like to thank to Prof. Junichi Segata, Associate Prof. Ryo Takada, Associate Prof. Pierluigi Cesana for their careful reading of my Ph.D thesis and their many insightful comments and suggestions.

Last but not the least, I would like to thank my parents, my brother and sisters who give me encouragement and support in my life.

Abstract

For an incompressible fluid, an interface of discontinuity in tangential velocity of a fluid in parallel motion is necessarily unstable, regardless to the strength of velocity difference. This is called the Kelvin-Helmholtz instability (KHI). The discontinuity in the tangential velocity signifies concentration of the vorticity at the interface. The vorticity spontaneously evolves into a distribution of enhancing the instability. Then Landau 1944 showed that the effect of compressibility on the stability weakens KHI. The growth rate of instability decreases with increasing of Mach number. If the ratio between velocity difference and the sound velocity satisfies equal or larger than value $\sqrt{8}$, the KHI is suppressed. There is an analogy between a compressible gas flow and a shallow water flow of an in compressible fluid. Bezdenkov and Pogutse (1983) studied the latter problem of stability of discontinuous surface in tangential velocity of shallow water of uniform depth, and obtained the same critical value $\sqrt{8}$ of the Froude number for suppressing the KHI.

In this thesis, we investigate the stability of a discontinuity interface in tangential velocity of a shallow-water flow. We focus on the effect of gravity waves on the KHI. We first consider the case of different depth in the regions separated by the interface. The propagation speed of the gravity wave depends on the depth. The difference in velocity of gravity waves on the two sides of interface has great influence of the stability. The critical value of the Froude number above which the KHI is completely suppressed takes the minimum value $\sqrt{8}$ for the equal depth. The critical. The critical value becomes larger as the depth ratio is larger or smaller from unity.

Second, we address the effect on the bottom friction. Without bottom drag, the interface of tangential-velocity discontinuity in the shallow-water flow is stable if the Froude number is greater than the critical value $\sqrt{8}$. However, the bottom friction plays significant roles in the linear stability of a two-dimensional shallow- water flow. Thereafter, we provide an example of the dissipation induced instabilities that are ubiquitous in nature. The instability persists in the regime of strong dissipation. We have obtained an unusual result that the instability mode is excited even for a large amount of dissipation; the discontinuity interface is linearly unstable over the entire range of drag coefficient as opposed to other models. In a closely related problem of a shear flow, only the effect of a small drag force was addressed.

For the preceding two problems, investigation is made of stability of an interface, of infinitesimal thickness, of discontinuity of tangential velocity. As the third problem, we address the stability of a shear layer, of finite thickness, sandwiched by infinite layers of uniform flows with different velocities. The simple shear, with the flow velocity a linear function of the normal coordinate, is assumed in the middle layer, for which eigenfunctions are written out in terms of the Whittaker functions and their derivatives. The similar is true for the dispersion relation for wavy deformations of two interfaces. We have confirmed that the appropriate limits of these functions are reduced to various known cases. The linear-shear layer of finite thickness totally alters the stability characteristics of the zero-thickness model. We show that the shear layer of finite thickness is linearly unstable for the entire range of the Froude number.

Contents

Notation

Acronyms

KHI	Kelvin Helmholtz Instability	1
SWE	Shallow Water Equation	10
2D	Two dimensions	12
3D	Three dimensions	52

Physical notation

$t, \delta t, \delta t_1$	the time and change of time in wave propagation	1
q	the horizontal wave number	4
U	Tangential-velocity difference in $x-$ direction	4
u	the fluid velocity in $x-$ direction	4
v	the fluid velocity in $y-$ direction	4
w	the fluid velocity in $z-$ direction	4
p	the pressure	4
ζ	the displacement at the interface	4
ρ	the mean density of fluid	6
ϕ	the velocity potential in region $z \geq 0$	6
p_1	the pressure in region $z \geq 0$ (or $y \geq 0$)	6
p_2	the pressure in region $z < 0$ (or $y < 0$)	6
ϕ_1	the velocity potential in region $z \geq 0$	6
ϕ_2	the velocity potential in region $z < 0$	6
K_1	the wave number in the region $z \geq 0$ (or $y \geq 0$)	8
K_2	the wave number in the region $z < 0$ (or $y < 0$)	8
M	the Mach number for a compressible fluid or Froud number for gravity wave	9
c	the sound velocity for compressible fluid or gravity velocity in a shallow water flow	8

g	the coefficient of gravity acceleration	2
H_0	the undisturbed depth of water	11
$\tilde{u}$	the perturbation of velocity in x direction	14
$\tilde{v}$	the perturbation of velocity in y direction	14
$\tilde{h}$	the perturbation of depth in a shallow water	14
H	the unperturbed depth in shallow water	14
H_1	the unperturbed depth in region $y \geq 0$ in the problem of depth difference	14
H_2	the unperturbed depth in region $y \geq 0$ in the problem of depth difference	14
c_1, c_2	the gravity-wave velocities corresponding to depth H_1, H_2	15
$\tilde{h}_{1,2}$	the perturbation of depth in region $y \geq 0,\ y < 0$ respectively	16
$\hat{\omega}$	the dimensionless of wave frequency	16
M_1, M_2	the Froude number corresponding to gravity velocity c_1, c_2	16
Ω	the transformation of variable $\hat{\omega}$	16
r	the ratio of depths H_1 and H_2 (ratio of gravity velocity)	16
$\zeta_{1,2}$	the displacement of the interface in region $y \geq 0,\ y < 0$ respectively	28
$\hat{q}$	the dimensionless wave number in $x-$ direction	37
$\hat{\omega}$	the dimensionless wave frequency in a problem of a simple shear layer	37
$\hat{y}, Y$	the transformation of variable y	37
τ	the parameter related to Whittaker function	37
α	the parameter related to Whittaker function	37
κ	the parameter of Whittaker functions	38
m	the parameter of Whittaker functions	38
$M_{\kappa,\pm}$	the Whittaker functions M	38
W	the transformation of function h_I	38
$\tilde{h}_I$	the perturbed depth in a simple shear layer	38

List of Figures

1. Instability of an interface of tangential - velocity discontinuity

1.1 Overview

Problems of stability of an interface between two fluids in a relative motion have received a wide interest of researchers of various fields. This type of instability is well known as the Kelvin-Helmholtz instability (KHI) which was first studied by Hermann von Helmholtz in 1868 and by William Thomson (Lord Kelvin) in 1871. The physical mechanism of KHI has been described by Batchelor (1967) [3] in term of the vorticity dynamics. The fluids are in a relative motion parallel to their interface, and the interface is necessarily unstable, regardless of the strength of different velocity. The discontinuity in the (tangential) velocity induces vorticity at the interface as a result, the shape of interface changes with time t and wiggly structure grows as shown in Figure 1.1

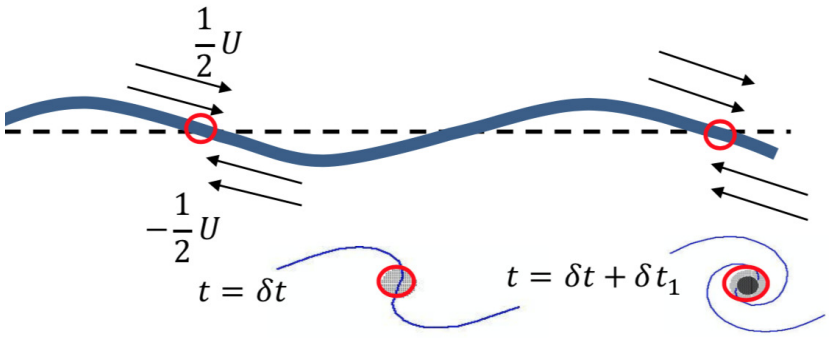

Figure 1.1: Creation of vorticity at the interface in the tangential velocity discontinuity

The instability of incompressible fluids was described by Lamb (1945) [23] which may be found earlier references. In the absence of gravity, surface tension and viscosity, the interface is unstable to all perturbations. The growth rate of instability is linear in wavenumber, with the coefficient proportional to velocity discontinuity.

The effect of compressibility on KHI was addressed by Landau (1944) [24] and the result of the incompressible case is drastically modified. He showed that the growth rate of instability decreases with the increasing of velocity difference. If the ratio of velocity difference to the sound velocity is equal or larger than $\sqrt{8}$, the interface of velocity discontinuity becomes stable. He also mentioned the analogy between the theory of a compressible gas and a shallow water of an incompressible fluid (see [25]).

Gill (1965) [16] studied the stability to a small disturbance of jets or wakes in a compressible fluid. A setting of a two-phase flow consists of a jet of compressible fluid shooting through another background of compressible fluid. Both cases of slag geometry and cylindrical jets model, he showed that the flow is unstable for entire values of Mach number.

Chang and Russell (1965) [10] have given the stability of the interface between an incompressible fluid and a flowing compressible fluid, including the effect of gravity, surface tension and viscosity. The effect of finite depth was supposed on the liquid layer in the inviscid case. They showed that the supersonic flow is always unstable while the subsonic flow is stable if the product between the gravity acceleration and the surface tension is greater than a certain value. When the liquid has a finite depth, these conclusions are unaltered. However, the supersonic flow is turned to be stable for a high viscous liquid when the gravity directs toward the denser liquid, and the subsonic flows still keep being stabilized under the same condition of inviscid case. All the conclusions of stability given by Chang and Russell are applied only to waves propagating along the flow direction.

Funada and Joseph (2001) [15] studied the stability of superposed uniform streams in a rectangular ducts using viscous potential flow. The effects of shear stress are neglected but the effects of normal stress are fully included. They showed that the effect of surface tension is disregarded for long waves while it is important for short waves. Amplification of short waves can be suppressed by increasing of surface tension. The comparison of theory and experiment for air-water flow was made to show that the effect of the normal stress is more important than the shear stress.

Landau and Lifshitz (1944) [25] also mentioned the analogy of theory of compressible gas flow (2D) with that of a shallow water of an incompressible fluid. Bezdenkov and Pogutse (1983) [6] was the first study of discontinuous surface in tangential velocity in an incompressible flow of shallow water since a shallow water flow in 2 dimensions has an analogy with a compressible gas flow. The geometry of stability problem is shown as Figure 1.2, the horizontal length scale is assumed much greater than the vertical length scale. The analogy of stability theory of compressible fluids with that of shallow water is limited to two dimensions because the hydrostatic balance is employed in the vertical direction and that we have to consider perturbations, with wavelength $\lambda \gg H$, where H is the depth of the fluid layer, depending only on the coordinates of the horizontal plane of the liquid layer (not on the depth coordinate z). The critical value of the Froude number $M = U/c$ for the interface stability was shown to be the same as in the case of a compressible fluids given by Landau [24]. The critical velocity is $\sqrt{8}c$, in which $c = \sqrt{gH}$, with g being the gravity acceleration, is the propagation speed of the gravity wave.

The stress in the horizontal plane stems from the bottom drag. For flood-wave equations of a shallow water, a uniform flow (or a uniform mean flow for a turbulent stream) can be linearly unstable. Further non-linear evolution of the disturbances typically leads to the formation of what are called roll waves; they have a finite amplitude and travel downstream. A criterion of linear instability of a one-dimensional flow was first obtained by Jeffreys (1925) [18] from the Saint Venant shallow-water equations. Later on several modifications and generalizations of the criterion and its proof were presented. Berlamont and Vanderstappen

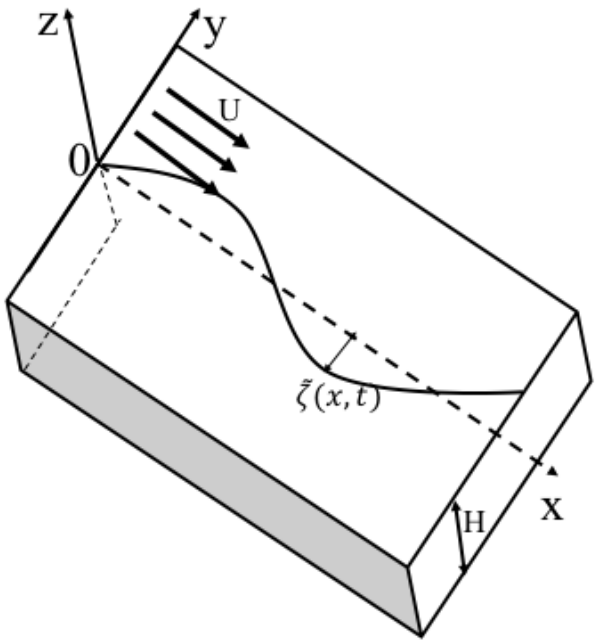

Figure 1.2: Shallow-water model for our stability problem. Perspective view of a shallow water flow of depth H. The basic state is a unidirectional flow, in the $x-$ direction, having velocity discontinuity along the $x-$ axis, with uniform velocity U for $y > 0$ and no flow for $y < 0$. The surface of discontinuity in tangential velocity is horizontally perturbed to $y = \zeta(x,t)$ with an infinitesimal amplitude.

[5] and Rosso *et al.* [33] analyzed the one-dimensional stability problem by means of the higher order long-wave approximation, i.e., the Boussinesq shallow-water equations. However, the internal lateral friction was disregarded in the analyses. On the contrary, Needham and Merkin (1984) [29] took into account the internal frictions but used the Saint Venant shallow-water equations. The problem of stability in shallow water has been revisited by Chen and Jirka (1997) [11] in connection with different geophysical applications.

A similar approach, based on the long-wave approximation, is often used in the dynamics of thin films. In contrast to flows of shallow water, film flows are typically laminar so that the fluid viscosity and the surface tension always play important roles. Criteria of linear instability for a laminar viscous flow on inclined plane, subjected to the gravity force, were derived from two- and three-dimensional Navier-Stokes equation by Benjamin (1957) [4] and Yih (1963) [45]. A review of more recent studies of three-dimensional instabilities in films has been presented by Liu et al [20]. Yakubenko and Shugai (1999) [44] analyzed the wave scattering problem and linear shear instability for the cases of small slope and the presence of bottom friction, and weak spanwise variation of the basic flow. The wave propagation was studied by means of the linearized Saint Venant shallow-water equations, endowed with the term for the bottom drag. However, the velocity profile of the basic flow and the bottom topography remain related uniquely by the bottom

friction.

Miles (1957) [28] and Ribner (1957) [32] were the first who studied the over-reflexion problem related to the transmission and reflexion of a sound waves at a vortex sheet separating by two regions of constant horizontal velocity U_1 and U_2. This problem was extended by Fejer (1963) [14] to include the hydromagnetic effect. Further, McKenzie (1972) [26] included the effects due to buoyancy. Jones (1968) [19] and Breeding (1971) [8] investigated numerically the over-reflection problem in an internal gravity waves meeting a vortex sheet which is separated by two uniform streams of an incompressible fluid. The same problem was considered analytically by Eltayeb and McKenzie (1975) [13]. Moreover, they wrote out the eigenfunctions in terms of the Whittaker function for the dispersion relation of wave perturbation in the shear layer which is sandwiched between two infinite layers in an incompressible fluid. Their results showed that wave amplification occurs if the Richardson number is less than the critical value 0.1129 approximately. Acheson (1976) [1] studied the over-reflection of hydromagnetic internal gravity waves propagating in an incompressible fluid and magneto-acoustic waves in a compressible fluid towards a vortex-current sheet. He also revealed quite clearly the energetic aspects of the over-reflexion mechanism, the reflected wave extracts energy from the mean motion and the sense in which the transmitted wave may be viewed as a carrier of so-called "negative energy" by analogy with certain concepts employed in plasma physics.

Vallis (2005) [38] considered the stability of the interface of non-zero thickness shear layer in an incompressible fluid. He showed that, for the single shear layer sandwiched by uniform flows, disturbances of long wavelength are amplified but those of short wavelength are no longer so.

In this thesis, we focus on the effect of gravity wave on an interface between two fluid regions which are moving parallel with different velocities in a shallow water flow. We first consider the effect of different depth in the regions separated by the interface as shown in chapter 2. In chapter 3, we address the effect on the bottom friction. We provide an example of the dissipation induced instabilities that are ubiquitous in nature. As the third problem, we investigate the stability of a shear layer, of finite thickness, sandwiched by infinite layers of uniform flows with different velocities

However, before studying the effect of gravity wave on the interface of tangential velocity discontinuity, we would like to revisit the instability of interface in an incompressible fluid, being well-known as the Kelvin-Helmholtz instability and the stability in a compressible fluid as given by Landau [25]. The last section of this chapter, we would like to introduce the shallow water equations which are derived from the Navier-Stokes equations.

1.2 Instability of a discontinuity interface in an incompressible fluid

An interface of the discontinuity in tangential velocity of an incompressible and inviscid fluid is subject to the instability, being well known as Kelvin-Helmholtz in-

stability; the interface is necessarily unstable, regardless of the strength of velocity difference.

Consider the surface of discontinuity, in the $z-$ direction, in tangential velocity and superpose a slight perturbation on it, in which pressure and fluid velocity are periodic functions, proportional to $e^{i(qx-\omega t)}$. Suppose that the fluid on the side $z \geq 0$ is moving with uniform velocity U, and that the fluid is at rest on the other side. The small perturbations in velocity for $z > 0$ denote to be (u_1, w_1) and the other side by (u_2, w_2). We assume that the density ρ is the same on the both sides of interface. For infinite depth, the flow geometry is shown in Figure 1.3. The

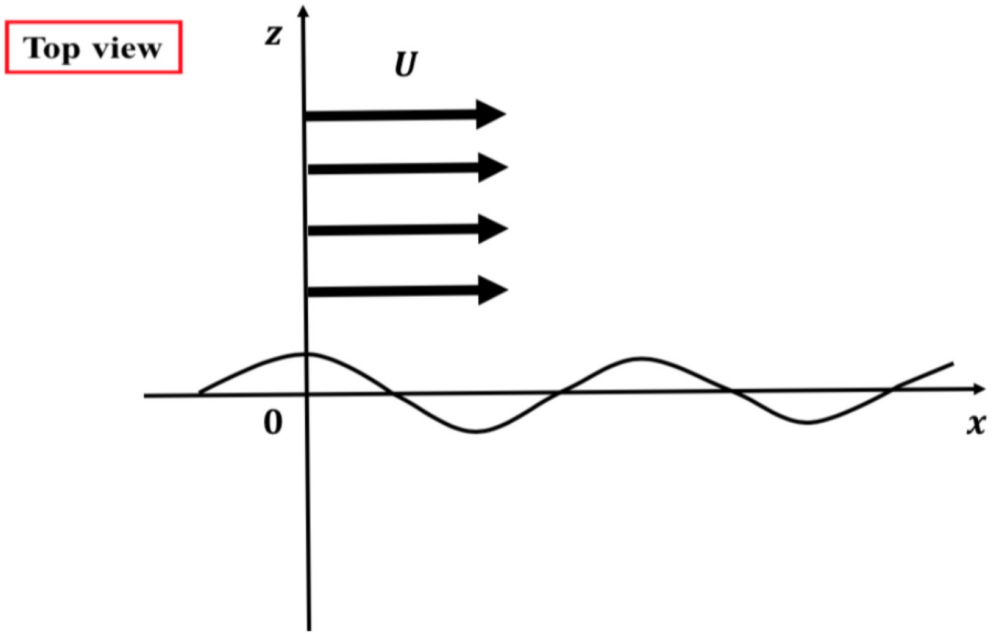

Figure 1.3: Top view of flow geometry for the linear instability problem of tangential-velocity discontinuity in the $x-$ direction, with uniform velocity U for $z > 0$ and no flow for $z < 0$.

momentum equations for a small perturbation are

$$\frac{\partial \mathbf{u}}{\partial t} + U_0 \frac{\partial \mathbf{u}}{\partial x} = -\frac{\mathbf{grad} p}{\rho}, \tag{1.1}$$

where, $U_0 = U$ for $z \geq 0$, $U_0 = 0$ for $z < 0$ and $\mathbf{u} = (u, w)$ is the velocity field.
The mass conservation equation for small perturbation is

$$\frac{\partial \rho}{\partial t} + \nabla \cdot (\rho \mathbf{u}) = 0. \tag{1.2}$$

We consider the linear perturbation of interface. Let $\zeta = \zeta(x, t)$ be the displacement in the $z-$ direction of points on the surface of discontinuity due to the perturbation. The derivative $\partial\zeta/\partial t$ is the rate of change of the surface coordinate ζ for a given value of x. Since the fluid velocity component normal to surface of discontinuity

is equal to the rate of displacement of the surface itself, we gain the kinematical boundary condition

$$\frac{\partial \zeta}{\partial t} + U_0 \frac{\partial \zeta}{\partial x} = w, \tag{1.3}$$

or,

$$\frac{\partial \zeta}{\partial t} + U_0 \frac{\partial \zeta}{\partial x} = \frac{\partial \phi}{\partial z}, \tag{1.4}$$

where, ϕ is the velocity potential. The momentum equations are integrated for the pressure disturbance in the form

$$p = -\rho\left(\frac{\partial \phi}{\partial t} + U\frac{\partial \phi}{\partial x}\right) \tag{1.5}$$

We impose the pressure to be equal on the surface of discontinuity and obtain the continuity condition

$$p_1 = p_2. \tag{1.6}$$

Since the fluids are incompressible, the mass conservation equation (1.2) becomes

$$\frac{\partial u}{\partial x} + \frac{\partial w}{\partial z} = 0. \tag{1.7}$$

We take divergence of both sides of momentum equations (1.1), the the left hand side gives zero by virtue of equation (1.7), so that pressure p must satisfy Laplace's equation:

$$\Delta p = 0. \tag{1.8}$$

We seek solution p in the form $p = f(z)e^{i(qx-\omega t)}$. Substitution into equation (1.8) yields equation for the function $f(z)$ as

$$\frac{d^2 f}{dz^2} - q^2 f = 0. \tag{1.9}$$

A general solution of this equation is given by $f = \text{constant} \times e^{\pm qz}$. Then in order to satisfy the condition of finiteness at infinity, we must take

$$\begin{aligned} p_1 &= f_1 e^{i(qx-\omega t)} e^{-qz} \quad (z > 0), \\ p_2 &= f_2 e^{i(qx-\omega t)} e^{qz} \quad (z < 0). \end{aligned} \tag{1.10}$$

The velocity potential is posed as

$$\begin{aligned} \phi_1 &= A_1 e^{i(qx-\omega t)e^{-qz}}, \\ \phi_2 &= A_2 e^{i(qx-\omega t)e^{qz}}. \end{aligned} \tag{1.11}$$

Substituting the expression of ϕ_1 into the equation (1.5), we find

$$p_1 = -[i(qU - \omega)]\phi_1. \tag{1.12}$$

On the other side of discontinuity surface, the quantities are given by a similar formula, where now $U = 0$ and ϕ_2 proportional to e^{qz}. Thus, the condition of equal pressure (1.6) at the tangential discontinuity reduces to

$$-[i(qU - \omega)]A_1 = [i\omega]A_2, \tag{1.13}$$

The displacement ζ can be obtained from equation (1.4), since the displacement ζ is assumed to be small, the value of w, of course, must be taken on the surface of discontinuity, i.e. at $z = 0$. This finally yields $w_{1z=0} = \partial\phi_1/\partial z = i(qU - \omega)\zeta$. This gives,

$$-qA_1 = i(qU - \omega)\zeta_0, \tag{1.14}$$

in which, ζ_0 is the amplitude of the displacement ζ. We obtain,

$$\begin{pmatrix} i(qU-\omega) & q & 0 \\ -i\omega & 0 & -q \\ 0 & i(qU-\omega) & i\omega \end{pmatrix} \begin{pmatrix} \zeta_0 \\ A_1 \\ A_2 \end{pmatrix} = 0. \tag{1.15}$$

For a nontrivial solution $(\zeta_0, A_1, A_2) \neq 0$ to exist, the determinant of the matrix in (1.15) must vanish, supplying the dispersion relation

$$(qU - \omega)^2 = -\omega^2. \tag{1.16}$$

Therefore, the dispersion relation between frequency ω and wave number q is solved for ω as

$$\omega = \frac{qU}{2}(1 \pm i). \tag{1.17}$$

We see that there is always one root ω having a positive imaginary part, for which the amplitude of the perturbation grows with time and we conclude that there is an instability. Thus, the tangential discontinuity interface is unstable, even with respect to infinite small perturbations. We note also that the frequency given by (1.17) has both real part and the imaginary part. It follows, in the case of Kelvin-Helmholtz instability, that perturbations propagate and at the same time grow in amplitude with the frequency

$$\mathrm{Re}[\omega] = \frac{qU}{2}, \tag{1.18}$$

and growth rate

$$\mathrm{Im}[\omega] = \frac{qU}{2}. \tag{1.19}$$

The growth rate is proportional to $x-$ component wave number q in the direction of flow so that the short waves grow the fastest. The growth rate of instability of tangential discontinuity surface depends on the different velocity U linearly. The instability is observed in the real world. For instance, the billow clouds, an array of spirals pattern, is manifestation of KHI (see Drazin (2002) [12]). The clouds are acting as tracers of fluid flow, indicating a shear in the atmosphere.

1.3 Instability of a discontinuity interface in a compressible fluid

Landau (1944) [25] showed that the Kelvin-Helmholtz Instability is suppressed by the effect of compressibility. In an incompressible fluid, the interface of tangential velocity discontinuity is necessarily unstable, regardless of the strength of velocity difference as shown in section 1.2. This section shows that the interface is stabilized

if the velocity difference U is large enough compared with the sound velocity c of a compressible fluid flow as given by Landau.

In compressible fluids, the main complicating factor is that we have to deal with sound waves for perturbed flow. The stability of the interface in a compressible fluid is drastically different from the incompressible case. The dispersion relation of wave frequency and other characteristics of a wave takes the form of a polynomial. The interface is stabilized if all roots of dispersion equation are real.

The equations of motion are in the form of (1.1) and (1.2). The momentum equations are integrated for the pressure disturbance in the form

$$p = -\rho(\frac{\partial \phi}{\partial t} + U_0 \frac{\partial \phi}{\partial x}). \tag{1.20}$$

The velocity potential is posed as

$$\begin{aligned} \phi_1 &= e^{i(qx-\omega t)}[A_1 e^{-K_1 z}], \\ \phi_2 &= e^{i(qx-\omega t)}[A_2 e^{K_2 z}], \end{aligned} \tag{1.21}$$

where A_1 and A_2 are constants. The displacement ζ is ruled by equation (1.4). Therefore, the kinematical boundary condition reduces to $w_1 = \partial\phi_1/\partial z = i(qU-\omega)\zeta$ on $z \approx 0$. This gives,

$$-K_1 A_1 = i(qU-\omega)\zeta_0, \tag{1.22}$$

in which, ζ_0 is the amplitude of the displacement ζ.

Substituting the expression of ϕ_1 into equation (1.5), we find the pressure perturbation as follow

$$p_1 = -[i(qU-\omega)]\phi_1 = -\frac{(qU-\omega)^2}{K_1}\zeta_0. \tag{1.23}$$

On the other side of discontinuity interface, the quantities are given by a similar formula, but now $U = 0$ and ϕ_2 proportional to $e^{K_2 z}$. The condition of equal pressure (1.6) on the interface reduces to

$$-\frac{(qU-\omega)^2}{K_1} = \frac{\omega^2}{K_2}, \tag{1.24}$$

In addition, we take divergence of both sides of momentum equations (1.1), and by using the equation of mass conservation (1.2), so that pressure p satisfies the following equation larger than Laplace's equation, *i.e.*,

$$\left(\frac{\partial}{\partial t} + U_0 \frac{\partial}{\partial x}\right)^2 p = c^2 \left(\frac{\partial^2}{\partial x^2} + \frac{\partial^2}{\partial z^2}\right) p, \tag{1.25}$$

in which, $c = \sqrt{p/\rho}$ is the speed of sound wave. From equation (1.25), we can easily obtain relation between $y-$ component of wave number K_1 (or K_2) and other quantities as

$$\begin{aligned} \left[-i(\omega - qU)^2\right] &= c^2(-q^2 + {K_1}^2), \\ (-i\omega)^2 &= c^2(-q^2 + {K_2}^2), \end{aligned} \tag{1.26}$$

or,

$$\begin{aligned} {K_1}^2 =& q^2 - \frac{(\omega - qU)^2}{c^2}, \\ {K_2}^2 =& q^2 - \frac{\omega^2}{c^2}. \end{aligned} \tag{1.27}$$

In the case $c \to +\infty$, relations (1.27) reduce to ${K_1}^2 = q^2, {K_2}^2 = q^2$ or $K_1 = K_2 = q$ which coincide with the ones in a flowing incompressible fluid as shown in section 1.2.

By taking square on both sides of equation (1.24) and then using relations in (1.27), we are led to the dispersion equation of ω, q, c and basic flow U as follows

$$\left[(\omega - qU)^2 - \omega^2\right]\left[\omega^2(\omega - qU)^2 - q^2c^2\left(\omega^2 + (\omega - qU)^2\right)\right] = 0. \tag{1.28}$$

This equation is decoupled into

$$\left[(\omega - qU)^2 - \omega^2\right] = 0, \tag{1.29}$$

and

$$\left[\omega^2(\omega - qU)^2 - q^2c^2\left(\omega^2 + (\omega - qU)^2\right)\right] = 0. \tag{1.30}$$

Solving equation (1.29) gives solution wave frequency ω as

$$\omega_0 = \frac{qU}{2}. \tag{1.31}$$

If we take the limit $c \to +\infty$, equation (1.30) returns to $\omega^2 + (\omega - qU)^2 = 0$, being the same with (1.16) as shown in section 1.2 for the case of incompressible fluid.

Solving equation (1.30) gives four other solutions as follows

$$\omega_{\pm,\pm} = \frac{q}{2}\left(U \pm \sqrt{U^2 + 4c^2 \pm 4c(U^2 + c^2)^{1/2}}\right). \tag{1.32}$$

The interface of velocity discontinuity is stabilized if all roots ω are real. This implies the term under square root in equation (1.32) to be non-negative, *i.e.*,

$$U^2 + 4c^2 - 4c(U^2 + c^2)^{1/2} \geq 0 \Leftrightarrow U \geq \sqrt{8}c. \tag{1.33}$$

The growth rate is proportional to $x-$ component wave number q in the direction of flow in the same way as in the incompressible fluid flow. But now, the growth rate depends on the ratio between different velocity U and the sound velocity c. The growth rate of instability is depicted in figure 1.4 as a function of the Mach number which is defined by ratio of velocity difference U to sound velocity c.

Figure 1.4 shows the growth rate of instability increases from 0 at $M = 0$ (there is no discontinuity velocity) to the maximum value $\mathrm{Im}[\omega] = 1$ at $M = \sqrt{3} \approx 1.72051$. Then, it decreases to zero at $M = \sqrt{8}$ as (1.33) shows. Moreover, all roots (1.32) are overlapped with the root (1.31) at $M = \sqrt{8}$. The growth rate vanishes for $M \geq \sqrt{8}$, i. e., the interface of tangential velocity discontinuity is stabilized.

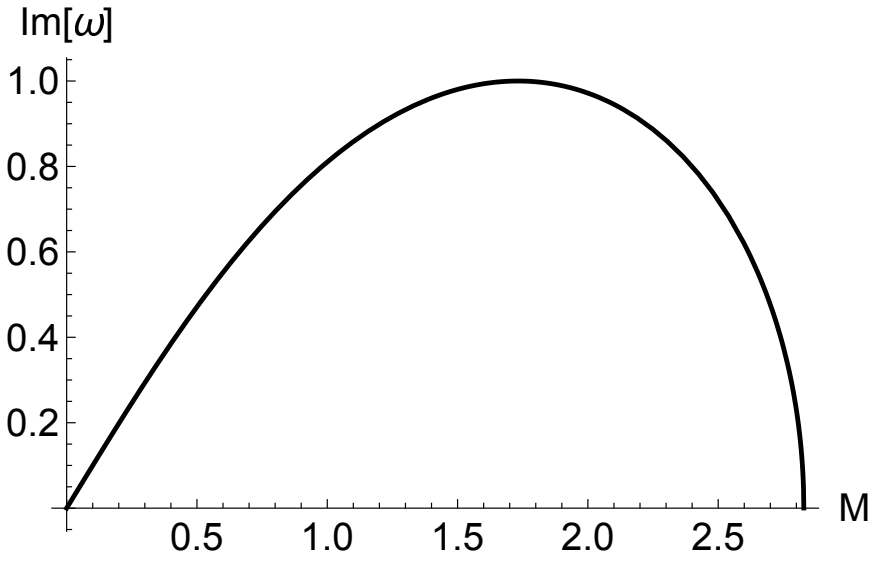

Figure 1.4: The growth rate $\mathrm{Im}[\omega]/q$ varies with the March number $M = U/c$ in the case of compressible fluids.

1.4 Derivation of Shallow-Water Equation

The shallow-water equations describe motion of a fluid in a thin layer of constant density in hydrostatic balance, bounded from below by the bottom topography and from above by a free surface. The shallow- water equations have applications to a wide range of phenomena other than water waves, e.g. avalanches and atmosphere flow. In this section, we derive the shallow water equations (SWE) by taking depth-average of theNavier-Stokes equation. The shallow-water equations are valid for problems in which the horizontal length scale is much greater than the vertical length scale so that the vertical dynamics can be neglected.

Here, we assume the fluid is inviscid, irrotational and incompressible. Using a control volume consisting of a vertical column of fluid, we derive the mass continuity equation. If ρ is the constant density of the fluid and h is the thickness of the fluid layer, ρh is the mass per unit area of fluid. The vertically integrated horizontal mass flux of fluid is $\rho h\mathbf{v}$ where $\mathbf{v} = (u, v)$ is the horizontal velocity and $\nabla = (\partial/\partial x, \partial/\partial y)$ is the horizontal gradient operator. Thus, the mass per unit time leaving a column of fluid of unit area $\nabla \cdot (\rho h\mathbf{v})$ is equal to minus the time tendency of the mass in this column $-\partial(\rho h)/\partial t$. Putting these facts together yields

$$\frac{\partial \rho h}{\partial t} + \nabla \cdot (\rho h\mathbf{v}) = 0. \tag{1.34}$$

The density is cancelled since it is nonzero constant. Equation (1.34) can be rewritten in advective form

$$\frac{Dh}{Dt} + h\nabla \cdot \mathbf{v} = 0, \tag{1.35}$$

in which

$$\frac{D}{Dt} = \frac{\partial}{\partial t} + \mathbf{v} \cdot \nabla. \tag{1.36}$$

We apply the Newton second law for a control volume in integral form to obtain the advective form, in the horizontal plane, for the averaged variables, as

$$\frac{D\mathbf{v}}{Dt} = -\frac{1}{\rho}\nabla p. \tag{1.37}$$

here the vertical component of the Coriolis force is ignored. Using the hydrostatic approximation, the pressure as a function of height is

$$p = -\rho g(d + h - z), \tag{1.38}$$

in which, $d(x, y)$ is the terrain elevation and we assume zero pressure at the upper fluid surface. Therefore, we have $\nabla p = -\rho g \nabla(d + h)$, and the momentum equation yields,

$$\frac{D\mathbf{v}}{Dt} + \rho g \nabla(d + h - z) = 0. \tag{1.39}$$

We assume that d is constant, set of equations (1.35) and (1.39) is the shallow water equations.

The depth h is represented as a constant average depth H_0 and a depth perturbation $\tilde{h}$ as

$$h = H_0 + \tilde{h}. \tag{1.40}$$

Then from the Navier-Stokes equation, we obtain the linearized shallow water equations in component wise as

$$\begin{aligned} \frac{\partial \tilde{h}}{\partial t} + H_0\left(\frac{\partial u}{\partial x} + \frac{\partial v}{\partial y}\right) &= 0, \\ \frac{\partial u}{\partial t} + g\frac{\partial \tilde{h}}{\partial x} &= 0, \\ \frac{\partial v}{\partial t} + g\frac{\partial \tilde{h}}{\partial y} &= 0. \end{aligned} \tag{1.41}$$

Posing a plane wave, in space and time, of the form $e^{i(qx+ky-\omega t)}$, (1.41) becomes

$$\begin{pmatrix} -i\omega & iqH_0 & ikH_0 \\ iqg & -i\omega & 0 \\ ikg & 0 & -i\omega \end{pmatrix}\begin{pmatrix} \tilde{h} \\ u \\ v \end{pmatrix} = 0. \tag{1.42}$$

We define the characteristic speed as

$$c = \sqrt{gH_0}. \tag{1.43}$$

We define the characteristic speed as

$$c = \sqrt{gH_0}. \tag{1.44}$$

For a non-trivial solution of (1.42), the determinant of the coefficient matrix equals zero, yielding the following equation

$$\left[\omega^2 - (q^2 + k^2)c^2\right]\omega = 0, \tag{1.45}$$

whose roots are

$$\omega = \pm c\sqrt{q^2 + k^2}, \text{ and } \omega = 0. \tag{1.46}$$

The shallow water system is two-dimensional, so that propagation of waves is purely horizontal with the wave phase speed $\omega/\sqrt{q^2 + k^2} = c$. The last solution, $\omega = 0$, is associated with steady balanced motion in the y-direction with no surface elevation $\tilde{h} = 0$. We do not consider this mode. The shallow water system is two-dimensional, so that propagation of waves is purely horizontal with the wave phase speed $\omega/\sqrt{q^2 + k^2} = c$. The last solution, $\omega = 0$, is associated with steady balanced motion in the y-direction with no surface elevation $\tilde{h} = 0$. We do not consider this mode.

Landau and Lifshitz (1944) [25] mentioned that there is an analogy between gravity waves in shallow-water flow of an incompressible fluid and sound waves in a compressible gas flow. There is a difference, however, because in the shallow-water case we have to consider perturbations depending only on the coordinates in the plane of the liquid layer (parallel and perpendicular to the velocity v), not on the depth coordinate z; the shallow-water approximation corresponds to perturbations with wavelength $\lambda \gg h$.

Exploiting this analogy, Bezdenkov and Pogutse [6] were the first who studied the stability of discontinuous surface in tangential velocity of an incompressible flow of shallow water. They obtained the critical value $\sqrt{8}$ of the Froude number for the interface stability by exploiting the analogy with the case of a compressible fluid. In the next chapters, we consider the effect of gravity waves on Kelvin-Helmholtz Instability of a shallow water flow. Three problems are investigated, namely, (i) different velocity of the gravity waves on the two sides of interface; (ii) the effect of frictional bottom; (iii) the effect of a simple shear layer sandwiched between two infinite layers, of finite thickness, moving parallel with different velocities. The well-known results of previous authors are recovered before going into the our final results and some new results are found.

2. Effect of depth difference on stability of an interface of tangential-velocity discontinuity of a shallow water

Landau and Lifshitz (1944) [25] mentioned that there is an analogy between gravity waves in shallow-water flow of an incompressible fluid and sound waves in a compressible gas flow. Exploiting this analogy, Bezdenkov and Pogutse (1984) [6] examined the instability of a tangential velocity discontinuity under conditions of shallow water as well where the phase speed of wave depends on the depth of water H. The perturbation along the $z-$ axis, is negligibly small compared to the scales λ of perturbations along the $x-$ and $y-$ axis . It was shown theoretically that the interface of a tangential-velocity discontinuity in a shallow water flow is stabilized if the condition of velocity difference $U \geq \sqrt{8gH}$ is satisfied, where g is the acceleration of gravity. In a shallow water flow, the characteristic velocity of gravity waves $c = \sqrt{gH}$, plays the role of the velocity of sound in a compressible fluid.

The purpose of this chapter is to address the effect of depth difference between two fluid regions, also known as the difference of gravity-wave velocity, on the linear stability of the interface of a tangential velocity discontinuity in a shallow water flow. Dispersion relation between wave frequency and other characteristics of wave is described in the form of a sextic polynomial, six roots for the complex wave-frequency are gained as functions of Froude number $M_1 = U/c_1$ and depth ratio $r = H_1/H_2$. The resulting dispersion relation is calculated numerically. The critical value of Froude number to make interface stability obtains as a function of depth ratio r. We find that the minimum of the critical Froude number $\sqrt{8}$ occurs at $r = 1$, that is, in the case of same depth. This coincides with the critical Froude number obtained by Bezdenkov and Pogutse [6].

Formulation of the problem is given and dispersion relation is derived in section 2.1. For clarity, the case of same depth [6] is revisited in section 2.2. Thereafter, we go into the effect of depth difference with asymptotic evaluations of depth ratio and by analyzing the dispersion relation numerically in section 2.3. The last section (section 2.4) gives a brief summary and discussions of this chapter.

2.1 Derivation of Dispersion equation

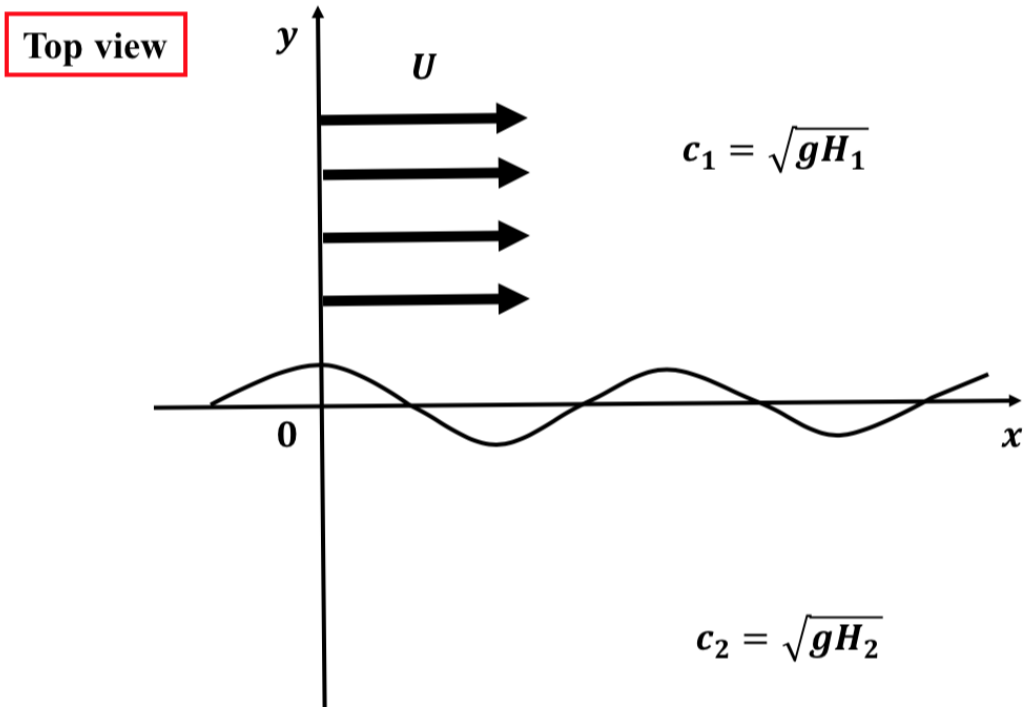

Figure 2.1: Flow geometry from the tope view of the linear instability problem of an interface of tangential-velocity discontinuity in a shallow water flow, in case of depth difference. The basic state is a unidirectional flow, in the $x-$ direction, having uniform velocity discontinuity U along $x-$ axis for $y > 0$ and no flow for $y < 0$. The fluid has gravity wave velocity c_1 in region $y > 0$ corresponding to the depth H_1 and be c_2 in region $y < 0$ corresponding to the depth H_2.

We consider the disturbances, of infinitesimal amplitude, $(\tilde{u}, \tilde{v})$ in the velocity field and $\tilde{h}$ in the height of the free surface (proportional to $e^{i(qx-\omega t)e^{-K_1 y}}$ for region $(y \geq 0)$, and $e^{i(qx-\omega t)e^{K_2 y}}$ for region $(y < 0)$, are superimposed as

$$\begin{aligned} u(x,y,t) &= U_0 + \tilde{u}(x,y,t), v(x,y,t) = \tilde{v}(x,y,t), \\ h(x,y,t) &= H + \tilde{h}(x,y,t), \end{aligned} \tag{2.1}$$

where,

$$U_0 = \begin{cases} 0 & y < 0 \\ U & y \geq 0 \end{cases}, \quad \text{and } H = \begin{cases} H_2 & y < 0 \\ H_1 & y \geq 0 \end{cases}. \tag{2.2}$$

The equations of motion and continuity equation in a shallow water flow have the following form

$$\begin{aligned} \frac{Dh}{Dt} + h(u_x + v_y) &= 0, \\ \frac{Du}{Dt} + gh_x &= 0, \\ \frac{Dv}{Dt} + gh_y &= 0. \end{aligned} \tag{2.3}$$

The linearized form for the small perturbation reads

$$\begin{aligned} &\frac{D\tilde{h}}{Dt} + H(\tilde{u}_x + \tilde{v}_y) = 0, \\ &\frac{D\tilde{u}}{Dt} + g\tilde{h}_x = 0, \\ &\frac{D\tilde{v}}{Dt} + g\tilde{h}_y = 0. \end{aligned} \tag{2.4}$$

Taking derivative of the last two equations (2.4) on x and y respectively, we have

$$\frac{D}{Dt}\left(\frac{\partial\tilde{u}}{\partial x} + \frac{\partial\tilde{v}}{\partial y}\right) + g\left(\frac{\partial^2}{\partial x^2} + \frac{\partial^2}{\partial y^2}\right)\tilde{h} = 0 \tag{2.5}$$

Substituting the first equation of (2.4) into equation (2.5), we obtain

$$\frac{D^2\tilde{h}}{Dt^2} - gH\left(\frac{\partial^2}{\partial x^2} + \frac{\partial^2}{\partial y^2}\right)\tilde{h} = 0. \tag{2.6}$$

We seek solution of depth perturbation in the form $\tilde{h}$ = constant $\times\, e^{\pm Ky}$, with $K = K_1$ or K_2 being wave number in $y-$ direction in the fluid regions $y \geq 0$ and $y < 0$ respectively. The signs of K_1 and K_2 is chosen corresponding to the inverse of the decay length in y direction.

In the region 1 $(y > 0)$, equation (2.6) gives

$$(-i(\omega - qU))^2 - gH_1(K_1^2 - q^2) = 0, \tag{2.7}$$

or,

$$K_1^2 = q^2 - \frac{(\omega - qU)^2}{c_1^2}, \text{ with } c_1 = \sqrt{gH_1}. \tag{2.8}$$

Similarly in the region 2 $(y < 0)$, we get

$$K_2^2 = q^2 - \frac{\omega^2}{c_2^2}, \quad \text{with } c_2 = \sqrt{gH_2}. \tag{2.9}$$

Here, c_1 and c_2 are known as velocity of gravity waves in regions $y \geq 0$ and $y < 0$ respectively.

We consider the linear perturbation of the interface, let $\zeta = \zeta(x,t)$ be the displacement in the $y-$ direction of points on the surface of discontinuity due to the perturbation. Since the normal component of the fluid velocity to surface of discontinuity is equal to the rate of displacement of the surface itself, we have necessarily the kinematical condition as

$$\frac{\partial\zeta}{\partial t} + U_0\frac{\partial\zeta}{\partial x} = \tilde{v} \quad \text{on } y = \zeta. \tag{2.10}$$

Since the displacement ζ is assumed to be small, the value of $\tilde{v}$, of course, must be taken on the surface of discontinuity, i.e. at $y = 0$. The kinematical condition (2.10) yields

$$\tilde{v}_{y=0} = \frac{\partial\zeta}{\partial t} + U_0\frac{\partial\zeta}{\partial x} \tag{2.11}$$

The horizontal displacement ζ of the interface is connected with the vertical one $\tilde{h}$ via

$$\begin{cases} gK_1\tilde{h_1} &= i(\omega - qU)^2\tilde{v} = (\omega - qU)^2\zeta, \\ gK_2\tilde{h_2} &= -i\omega^2\tilde{v} = -\omega^2\zeta, \end{cases} \quad \text{on } y = \zeta \tag{2.12}$$

The pressure should be continuous across the discontinuity surface. In the hydrostatic approximation, the pressure perturbation $\tilde{p}$ is equal $\rho g\tilde{h}$, and this dynamical boundary condition is reduced to that of the continuity of the wave height across the interface:

$$\tilde{h_1} = \tilde{h_2} \text{ at } y \approx 0. \tag{2.13}$$

This condition reduces to

$$\frac{K_1}{K_2} = -\frac{(\omega - qU)^2}{\omega^2}. \tag{2.14}$$

We arrive at the desired dispersion relation between the complex frequency ω and other characteristics of wave as follows

$$\frac{q^2 - (\omega - qU)^2/c_1^2}{q^2 - \omega^2/c_2^2} = \frac{(\omega - qU)^4}{\omega^4}, \tag{2.15}$$

or

$$\left[q^2 - \frac{(\omega - qU)^2}{c_1^2}\right]\omega^4 - \left[q^2 - \frac{\omega^2}{c_2^2}\right](\omega - qU)^4 = 0. \tag{2.16}$$

For dimensionless variables

$$\hat{\omega} = \frac{\omega}{qU}, \quad M_1^2 = \frac{U^2}{c_1^2}, \quad M_2^2 = \frac{U^2}{c_2^2}. \tag{2.17}$$

Dispersion equation of dimensionless of wave-frequency variable $\hat{\omega}$ yields,

$$\left[1 - M_1^2(\hat{\omega} - 1)^2\right]\hat{\omega}^4 - \left(1 - M_2^2\hat{\omega}^2\right)(\hat{\omega} - 1)^4 = 0. \tag{2.18}$$

We set

$$\Omega = \hat{\omega} - 1/2, \quad r = \frac{M_2^2}{M_1^2} = \frac{H_1}{H_2}, \tag{2.19}$$

then equation (2.18) turns to

$$\left(1 - M_1^2(\Omega - 1/2)^2\right)(\Omega + 1/2)^4 - \left(1 - rM1^2(\Omega + 1/2)^2\right)(\Omega - 1/2)^4 = 0. \tag{2.20}$$

We write this equation in the standard form of polynomial

$$\begin{aligned} f(\Omega) = (r-1)\Omega^6 - (r+1)\Omega^5 - \frac{(r-1)}{4}\Omega^4 + \left(\frac{(r+1)}{2} + \frac{4}{M_1^2}\right)\Omega^3 - \frac{(r-1)}{16}\Omega^2 \\ + \left(\frac{1}{M_1^2} - \frac{r+1}{16}\right)\Omega + \frac{(r-1)}{64} = 0. \end{aligned} \tag{2.21}$$

The dispersion relation between dimensionless wave-frequency Ω and other characteristics of wave (2.21) is a sextic polynomial equation of Ω which has six roots $\Omega_k(k = \bar{1,6})$. Since M_1, r are real numbers, then all coefficients of polynomial are real number, too. Therefore, if this equation has a complex root then the conjugate

complex of that root is root of equation. In other words, the interface is stabilized if and only if, this equation has all six real roots. In the case $r > 1$, we see polynomial $f(\Omega)$ has four times of change of sign and $f(-\Omega)$ has two times of change of sign. Therefore, using *Descartes's Rule Sign*, equation (2.21) has either four, two or zero positive real roots and either two or zero negative real roots. Similarly, in the case $r < 1$, $f(\Omega)$ changes sign two times and $f(-\Omega)$ changes sign four times, $f(\Omega) = 0$, has either two or zero positive real roots and either four or two or zero negative real root. We are going to find complex roots of equation $f(\Omega) = 0$ which are conjugate complex number of each other. If at least one of the complex roots has positive imaginary part, then interface is destabilized and hereafter we denote Ω_{max} as the root with maximum positive imaginary part, that induces an unstable mode with maximum growth rate.

To be convenient in either recovering a well-known result or analyzing asymptotically later, we rewrite equation (2.21) in the following form

$$\begin{aligned}(\Omega+1/2)^4-(\Omega-1/2)^4-M_1^2(\Omega-1/2)^2(\Omega+1/2)^2\left[(\Omega+1/2)^2-(\Omega-1/2)^2\right]\\ =M_1^2(1-r)(\Omega-1/2)^4(\Omega+1/2)^2.\end{aligned} \tag{2.22}$$

2.2 Case of same depth

Before looking into the effect of depth difference, we review the case of the same depth $H_1 = H_2 = H$ or $r = 1$ as considered by Bezdenkov and Pogutse. In this case, the sextic equation of dispersion relation (2.22) switches to a quintic equation as follows

$$\begin{aligned}&(\Omega+1/2)^4-(\Omega-1/2)^4-M_1^2(\Omega-1/2)^2(\Omega+1/2)^2\left[(\Omega+1/2)^2-(\Omega-1/2)^2\right]=0\\ &\qquad\Longleftrightarrow \Omega\left[(\Omega+1/2)^2+(\Omega-1/2)^2-M_1^2(\Omega^2-1/4)^2\right]=0\\ &\text{devides by } M_1^2 \iff \Omega\left[\Omega^4-(\frac{1}{2}+\frac{2}{M_1^2})\Omega^2+\frac{(M_1^2-8)}{16M_1^2}\right]=0.\end{aligned} \tag{2.23}$$

We obtain solutions of this equation as follows

$$\begin{aligned}\Omega_0^0 &=0,\\ \Omega_{\pm,\pm}^0 &= \pm\left[\frac{1}{4}+\frac{1}{M_1^2}\pm\frac{(M_1^2+1)^{1/2}}{M_1^2}\right]^{1/2}.\end{aligned} \tag{2.24}$$

The interface is stabilized if

$$\frac{1}{4}+\frac{1}{M_1^2}-\frac{(M_1^2+1)^{1/2}}{M_1^2}\geq 0$$

or $M_1^2 \geq 8$. The solid line in Figure 2.2 presents the variation of the growth rate of instability with Froude number M_1. The instability decreases with an increasing Froude number, the interface is stabilized corresponding to the imaginary part of wave frequency $\mathrm{Im}[\Omega_{-,-}^0] = 0$ at $M_1 \geq \sqrt{8}$. This condition of stability coincides with the result of Bezdenkov [6] in shallow water and result of Landau [25] for compressible fluids in two dimensions.

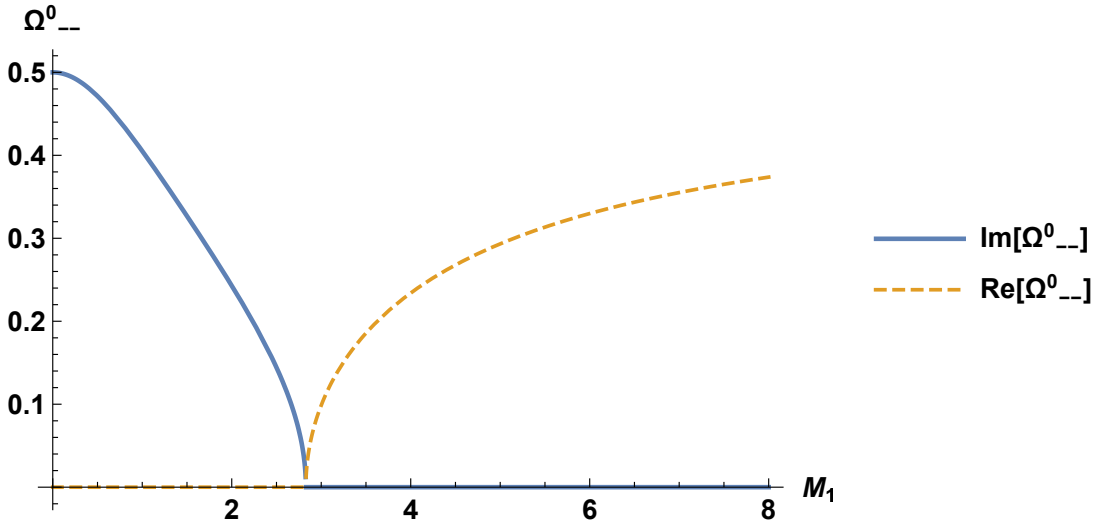

Figure 2.2: Real part (dashed) and Imaginary part (solid) of $\Omega^0_{\_,\_}$ in equation (2.24) with given $r = 1$ as considered by Bezdenkov and Pogutse (1984). The solid line describes the growth rate of unstable mode with the Froude number M_1. The growth rate decreases with an increasing Froude number, and vanishes at $M_1 = \sqrt{8}$, i.e., the interface stability.

2.3 Effect of depth difference

In this section, we show how the critical value of Froude number $\sqrt{8}$ in case of same depth considered by Bezdenkov and Pogutse [6] is modified asymptotically and numerically.

In case $M_1 \to \infty$ or $r \to 0$, (i.e. $H_1 \to 0$), dispersion equation (2.21) yields,

$$\begin{aligned} f(\Omega) =& \Omega^6 + \Omega^5 - \frac{1}{4}\Omega^4 - \frac{1}{2}\Omega^3 - \frac{1}{16}\Omega^2 + \frac{1}{16}\Omega + \frac{1}{64} = 0 \\ \Longleftrightarrow& \frac{1}{64}(2\Omega - 1)^2(2\Omega + 1)^4 = 0. \end{aligned} \tag{2.25}$$

We see that all roots of this equation are real, i.e., $\Omega = \pm\frac{1}{2}$. This satisfies the stability condition of interface. However, in the view of fluid mechanics, H_1 (or H_2) has a physical meaning as the depth of water in the region $y > 0$ (or $y < 0$) respectively. If $r \to 0$ (*i.e.* $H_1 \to 0$), the model is one side flow. It is similar for the case $r \to \infty$ meant to $H_2 \to 0$. Therefore, we will not consider these cases any longer.

Next, we consider he effect of depth difference between two fluid regions and then compare with the critical value $M_{1c} = \sqrt{8}$ as given by Bezdenkov and Pogutse [6]. For the purpose of fundamental knowledge, we assume $(r-1) \ll 1$, so that we may approximate the dispersion equation (2.21) as the following equation:

$$(r+1)\Omega^5 - \left(\frac{(r+1)}{2} + \frac{4}{M_1^2}\right)\Omega^3 - \left(\frac{1}{M_1^2} - \frac{r+1}{16}\right)\Omega \approx 0. \tag{2.26}$$

This equation has five roots $\tilde{\Omega}$ as follow.

$$\begin{aligned}\tilde{\Omega}_0 =& 0,\\ \tilde{\Omega}_{\pm}^2 =& \frac{1}{4} + \frac{2}{M_1^2(1+r)} \pm \frac{\sqrt{4+2M_1^2(1+r)}}{M_1^2(1+r)}.\end{aligned} \tag{2.27}$$

The interface is stabilized if only if all roots $\tilde{\Omega}$ of (2.26) are real. This condition reduces $\tilde{\Omega}_{\pm}^2 \geq 0$ or $M_1^2(r+1) \geq 16$.

Figure 2.3 shows the contours of $\tilde{\Omega}_{\pm}^2$ plot for the different Froude number M_1 and depth ratio r. The region with positive-value contours corresponds to $\tilde{\Omega}_{\pm}^2 > 0$ which reduce to $\tilde{\Omega}_{\pm,\pm}^2 0$ real. In this region, the interface is stabilized, in the other the interface is destabilized. This condition reduces to the critical value $M_c \geq \sqrt{8}$ if depth ratio $r = 1$ or $H_1 = H_2$ as same as shown in equation (2.24).

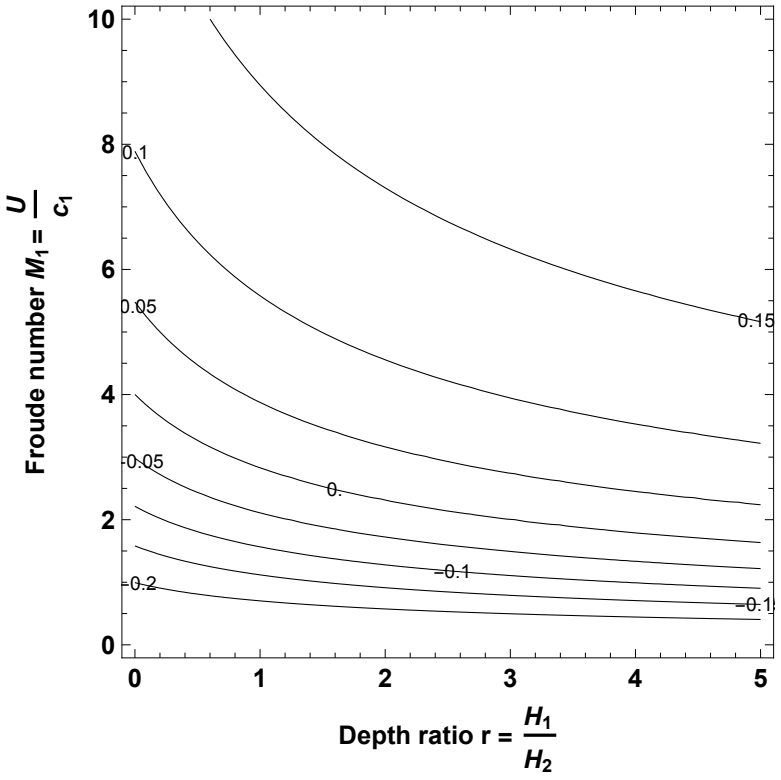

Figure 2.3: The variation $\tilde{\Omega}_{\pm}^2$ contour in equation (2.27) plots for different Froude number $M_1 = U/c_1$ and depth ratio r of H_1 to H_2 in case $(r-1) \ll 1$.

To gain insight in the effect of depth difference, we express the root of (2.24) in a power series in a small factor $(r-1)$ to first order as $\Omega = \Omega^0 + (r-1)\hat{\Omega}$, in which Ω^0 is given by equation (2.24) and the correction term

$$\hat{\Omega} = \frac{M_1^2(2\Omega_0 - 1)^4(2\Omega_0 + 1)^2}{4\left[M_1^2(80\Omega_0^4 - 24\Omega_0^2 + 1) - 96\Omega_0^2 - 8\right]} \tag{2.28}$$

We see that $\hat{\Omega}$ is always real for Ω_0 real. Figure 2.4 shows the variation of imaginary part of $\hat{\Omega}$ with Froude number $0 < M_1 < \sqrt{8}$ corresponding to the case Ω_0 is pure

imaginary. The growth rate of instability $\mathrm{Im}[\Omega]$ is the sum of $\mathrm{Im}[\Omega_0]+(r-1)\mathrm{Im}[\hat{\Omega}]$.

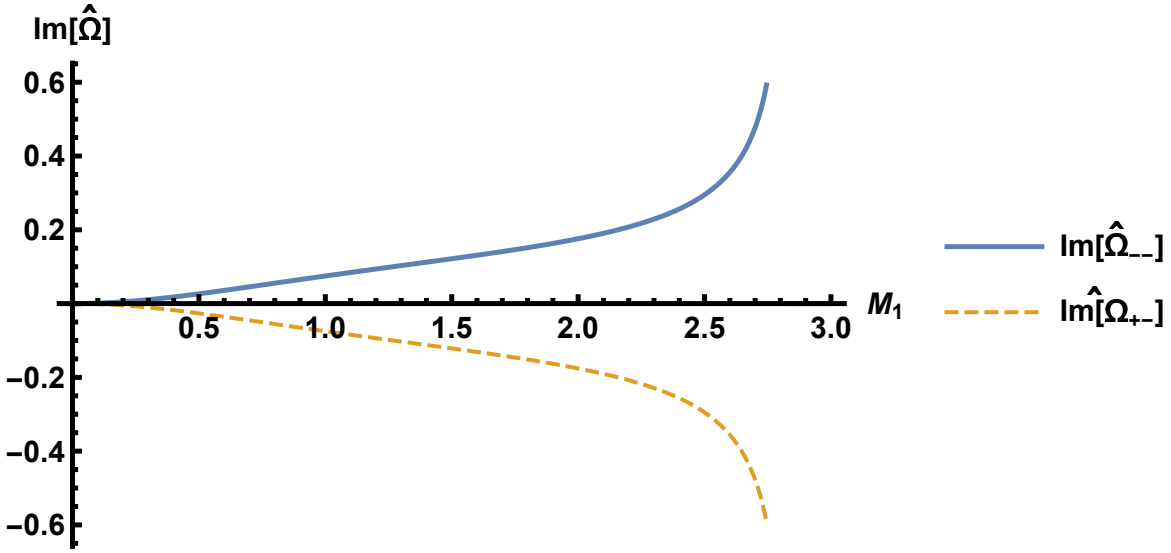

Figure 2.4: The leading order of growth rate $\mathrm{Im}[\hat{\Omega}]$ in equation (2.28) is a function of Froude number $0 < M_1 < \sqrt{8}$ for the case $(r-1) \ll 1$. Solid line corresponds to an unstable mode, dashed line is for a stable mode.

In the general case, and $r \neq 1$, the six roots of dispersion equation (2.21) depend on two variables r and M_1. We can reduce dispersion equation (2.21) to the equation of $M_1^2 = g(\Omega, r)$ as follows

$$M_1^2 = g(\Omega, r) = -\frac{64\Omega(4\Omega^2+1)}{(1-4\Omega^2)^2\left[4(r-1)\Omega^2 - 4(r+1)\Omega + (r-1)\right]}. \tag{2.29}$$

Easily, we can see the denominator of $g(\Omega, r)$ goes to zero at $\Omega = \pm 1/2$ and $\Omega = (\sqrt{r} \pm 1)^2/2(r-1)$. In case $r > 1$, the denominator of function g has a negative sign if $\Omega \in \left[\frac{(\sqrt{r}-1)^2}{2(r-1)}, \frac{(\sqrt{r}+1)^2}{2(r-1)}\right]$ or has a positive sign if $\Omega \notin \left[\frac{(\sqrt{r}-1)^2}{2(r-1)}, \frac{(\sqrt{r}+1)^2}{2(r-1)}\right]$. In case $0 < r < 1$, the denominator of function g has a positive sign if $\Omega \in \left[\frac{(\sqrt{r}+1)^2}{2(r-1)}, \frac{(\sqrt{r}-1)^2}{2(r-1)}\right]$ or has a negative sign if $\Omega \notin \left[\frac{(\sqrt{r}+1)^2}{2(r-1)}, \frac{(\sqrt{r}-1)^2}{2(r-1)}\right]$. Therefore, for a given r, there are six branches of $g(\Omega, r) \to +\infty$. In other words, if M_1^2 is large enough, the equation $M_1^2 = g(\Omega, r)$ will have six real roots $M_{1k}^2(\Omega, r), k = \bar{1,6}$. Then we can reduce all six real roots Ω_k of dispersion equation (2.21) from the roots M_{1k} of equation (2.29).

For numerical results, we separate into two cases $0 < r < 1$ and $r > 1$, corresponding to $H_1 < H_2$ and $H_1 > H_2$. The critical value M_{1c} for all six roots of (2.21) real (*i.e.* the interface stability) is a function of depth ratio r. In case $0 < r < 1$, the critical value of Froude number M_{1c} for the interface stability is a decreasing function of depth ratio r. But the critical value is an increasing function of the depth ratio r in the case $r > 1$. Both these cases, the critical Froude number M_{1c} is still greater than $\sqrt{8}$. Figures 2.5 describes graphs of the critical value M_{1c} of Froude number as a function of depth ratio r. Figure 2.5 shows the minimum of

critical value is $\sqrt{8}$ at $r = 1$ corresponding to the case of same depth as considered by Bedenzkov [6].

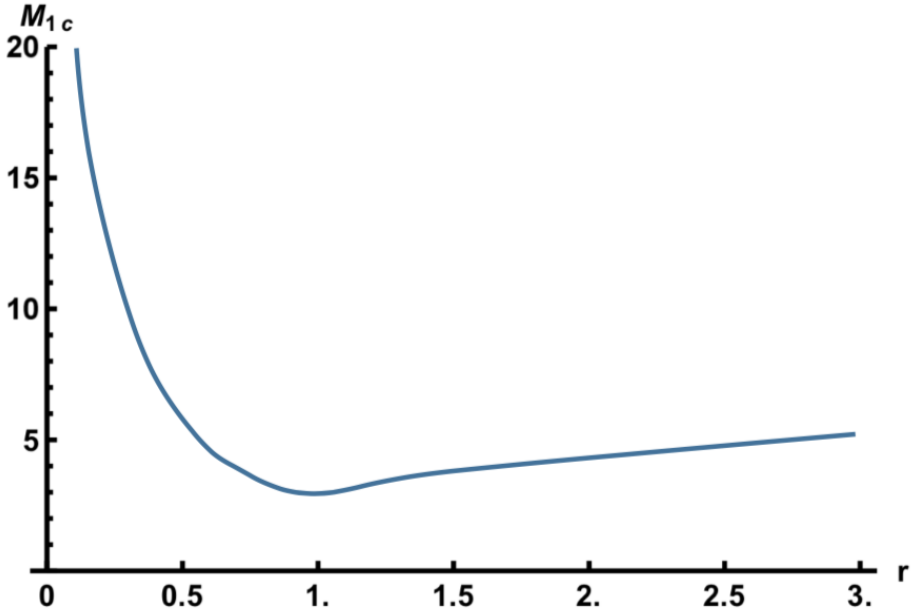

Figure 2.5: Graph of the critical value M_{1c} of Froude number is a function of depth ratio r. The minimum of the critical Froude number occurs at $r = 1$ with the critical value $M_{1c} = \sqrt{8}$ as same as the case considered by Bezdenkov and Pogutse.

Figures 2.6 and (2.7) display contours of the maximum growth rate of instability for different Froude number M_1 and depth ratio r of H_1 to H_2, also known as the ratio of gravity-wave velocity c_1 to c_2. Figure 2.8 describes the variation of maximum growth rate corresponds to $\mathrm{Im}[\Omega_{max}]$ (which has maximum imaginary part) on Froude number $M_1 > 0$ with four given values of depth ratio $r = 1, 2, 3, 4$. Figure 2.9 presents the variation of maximum growth rate on Froude number $M_1 > 0$ with four given values of depth ratio $r = 0.1, 0.2, 0.3, 0.4$. So that the instability perturbations both propagate and grow in amplitude with the frequency $\mathrm{Re}[\Omega_{max}]$ and growth rate $\mathrm{Im}[\Omega_{max}]$. When M_1 is large enough, imaginary part $\mathrm{Im}[\Omega_{max}]$ decreases to zero corresponding to a stable mode, i.e., the interface of tangential-velocity discontinuity is stabilized.

Numerically, we find that the critical value M_{1c} which makes interface stability is greater than $\sqrt{8}$ if $r \neq 1$. In case $r > 1$ the critical value of Froude number M_{1c} increases if r decreases while M_{1c} increases if r increases in the case $0 < r < 1$. This can be seen in Figures 2.5, 2.6 and 2.7.

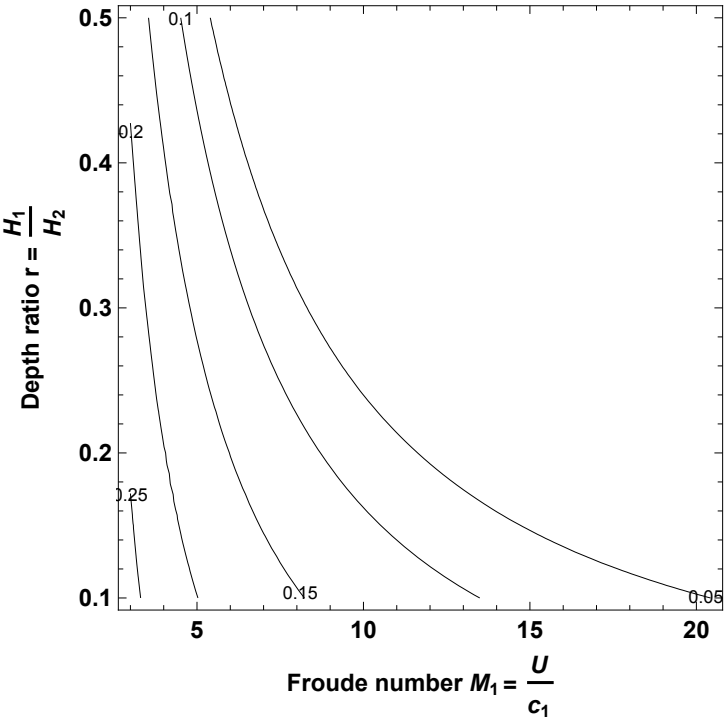

Figure 2.6: Maximum growth rate contour plot for different Froude numbers M_1 and depth ratio $0 < r < 1$.

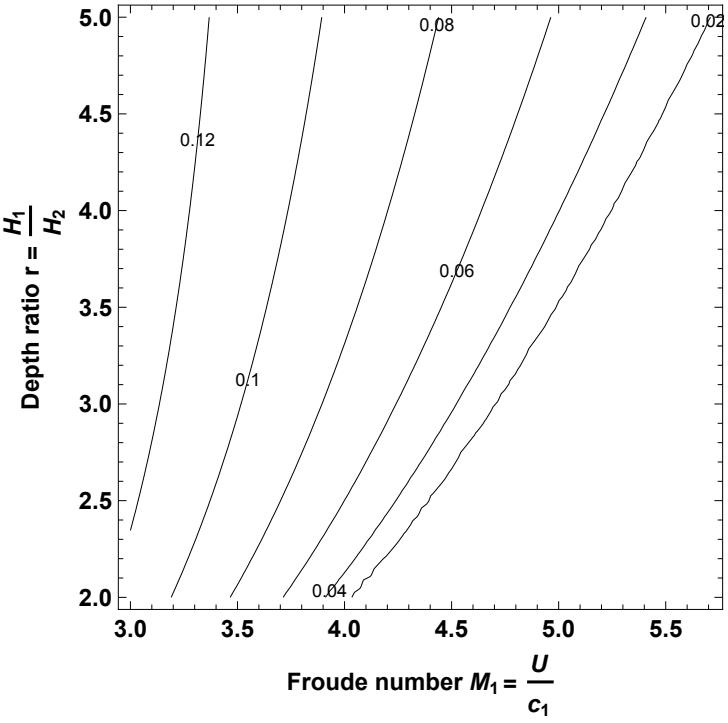

Figure 2.7: Maximum growth rate contour plot for different Froude numbers M_1 and depth ratio $r > 1$.

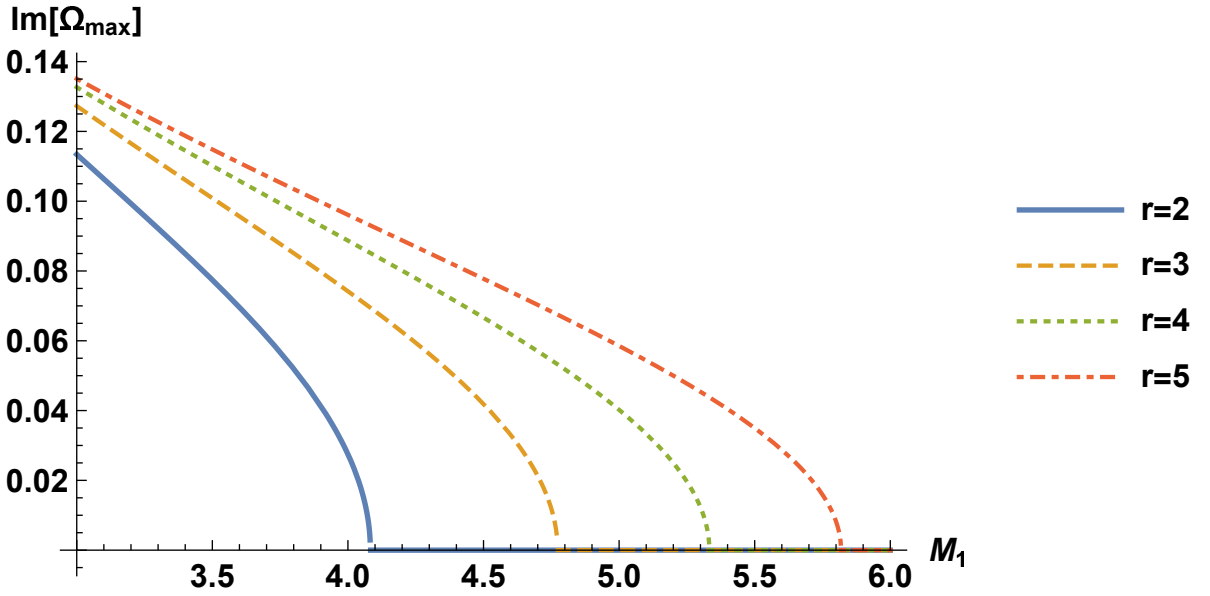

Figure 2.8: The maximum growth rate of instability varies with Froude number M_1 for four given values of depth ratio $r = 2, 3, 4, 5$. The critical value of Froude number M_1 which $\mathrm{Im}[\Omega_{max}]$ starts being zero (the growth rate vanishes), is increasing with the increment on r.

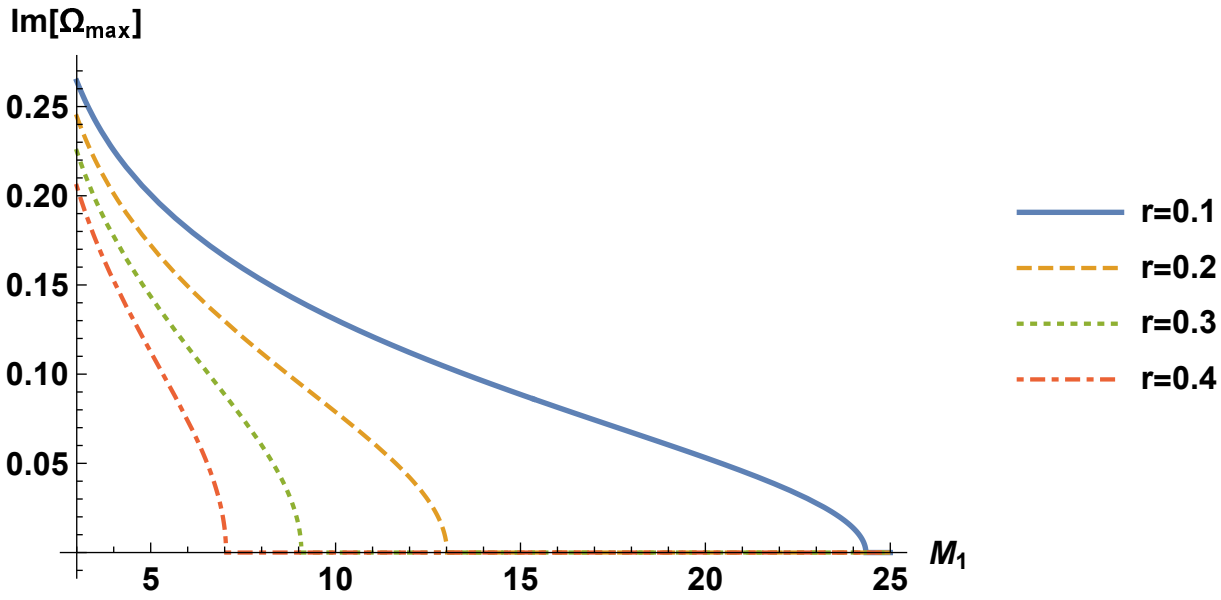

Figure 2.9: The maximum growth rate of instability varies with Froude number M_1 for four given values of depth ratio $r = 0.1, 0.2, 0.3, 0.4$. The critical value of Froude number M_1 which $\mathrm{Im}[\Omega_{max}]$ starts being zero (the growth rate vanishes), is increasing with the decrement on r.

2.4 Discussion

We have considered the linear stability problem of an interface of tangential-velocity discontinuity in shallow water, including the effect of depth difference on the both sides of interface. We obtained the dispersion relation between the wave frequency ω and the other characteristics of wave as a sextic polynomial. In case $r = 1$ for a same depth as considered by Bezdenkov and Pogutse [6], the dispersion equation is altered to the quintic polynomial equation. The critical value of Froude number is $\sqrt{8}$ for the interface stability. In the general cases and $r \neq 1$, the critical value M_{1c} varies with the depth ratio r as shown by Figure 2.5. The critical value M_{1c} was an increasing function with $r > 1$ and was a decreasing function for $0 < r < 1$. For the both of cases r, the critical value M_{1c} is always greater than $\sqrt{8}$. Our results show that interface is stablized if the Froude number $M_1 = U/c_1$ satisfies equal or greater than the critical value M_{1c}.

3. Effect of bottom drag on on stability of an interface of tangential-velocity discontinuity of a shallow water

The linear stability of a surface of tangential-velocity discontinuity in a shallow water along a frictionless horizontal plane had an exact analytic solution for small disturbances by Bezdenkov and Pogutse [6]. They showed that the interface is stable if the Froude number is large enough compared with the gravity wave. The critical value $\sqrt{8}$ of Froude number for interface stable is coincided with the one obtained by Landau (1944) [24] for a compressible fluid. This analogy was mentioned by Landau and Lifshitz (1944) [25]. However, the bottom friction and the internal lateral friction both play significant roles in the linear stability of a two-dimensional shallow- water flow. The analysis is based on the Boussinesq shallow-water equations, this category of instability is usually considered for a small amount of dissipation. The instability persists in the regime of strong dissipation. In this chapter, we show how this solution of Bezdenkov and Pogutse can be adapted for a more realistic flow of shallow water, for which the bottom friction is not negligible. Because of the shallowness of fluid layer, the shallow water flow is liable to be acted by the bottom drag. The frictional force may well be considered as a stabilizing factor, but there are cases where the drag force causes the instability, being known as the dissipation induced instability[21, 30]. Even a small friction is suffice to cause the instability.

The dispersion relation is obtained by enforcing the boundary conditions at the discontinuity surface, from which the stability characteristics is deduced. Six roots for the complex frequency ω, of the dispersion equation, are gained as functions of the discontinuity velocity U, the traveling speed c of the gravity wave and the drag coefficient γ. The resulting dispersion relation is calculated numerically. An asymptotic evaluation of the roots are made for both small and large values of the drag coefficient γ.

For clarity, we will revisit the result given by Bedenzkov and Pogutse [6] to obtain The critical value of Froude number $M = U/c = \sqrt{8}$ in the case of no frictional bottom in Sec. 3.2. Thereafter in Sec. 3.3, we go into the influence of the bottom drag. The last section (Sec. 3.4) is devoted to a summary and conclusions.

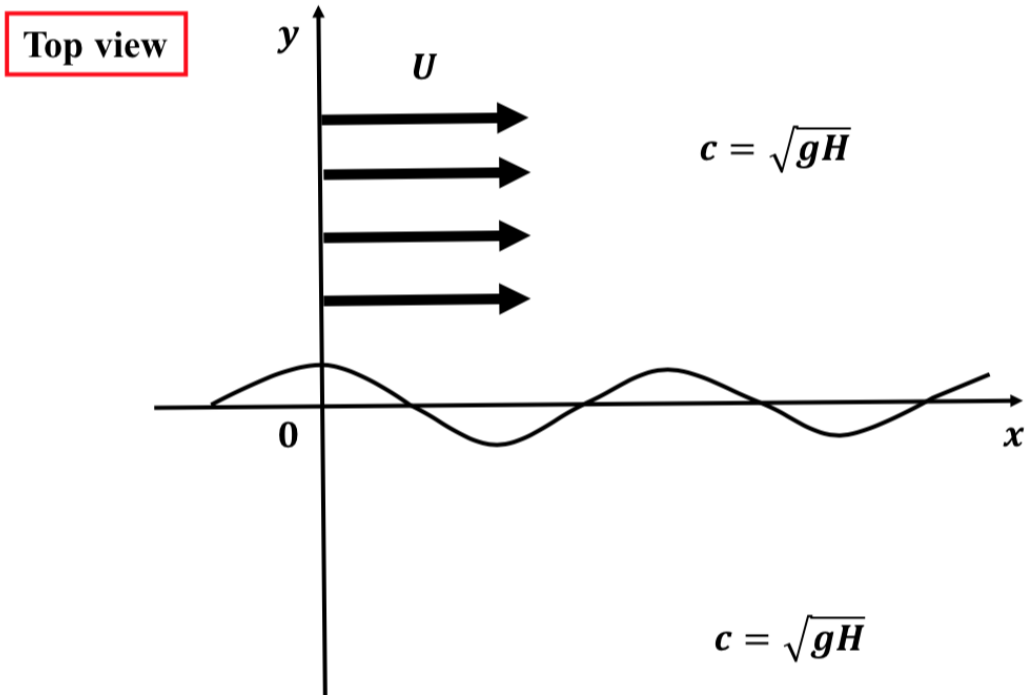

Figure 3.1: Flow geometry from the tope view of the linear instability problem of tangential-velocity discontinuity in a shallow water flow, including the effect of the frictional bottom. The basic state is a unidirectional flow, in the $x-$ direction, having uniform velocity U along $x-$ axis for $y > 0$ and no flow for $y < 0$. The model is assumed to have the same depth H on the both sides of the interface.

3.1 Formulation of problem and dispersion relation

We begin with the shallow-water equations with drag force taken into account in the momentum equations. For the basic state, we take the interface along the x axis, with the water flowing, with a uniform velocity U, in the x direction for $y > 0$, while at rest on the other side ($y < 0$) as shown in Figure 3.1.

Consider long waves, with infinitesimal wave amplitude a, on a shallow water, with the horizontal length scale significantly longer than the water depth H. The governing equations for the shallow-water stream are derived by taking averages of the three-dimensional motion, over the depth, of the flow in a thin layer with a free surface elevation given by $z = h(x, y, t)$ in Cartesian coordinate system (x, y, z):

$$\begin{aligned} &\frac{Dh}{Dt} + h(u_x + v_y) = 0, \\ &\frac{Du}{Dt} + gh_x = -\gamma u\sqrt{u^2 + v^2} + S(x, y), \\ &\frac{Dv}{Dt} + gh_y = -\gamma v\sqrt{u^2 + v^2}, \end{aligned} \tag{3.1}$$

where a subscript stands for derivative with respect to the indicated variable and

D/Dt denotes the Lagrange derivative

$$\frac{D}{Dt} = \frac{\partial}{\partial t} + u\frac{\partial}{\partial x} + v\frac{\partial}{\partial y},$$

and the salt term $S(x, y)$ (see Whitham, 1974) [42] is assumed to be constant as follow:

$$S(x, y) = \begin{cases} \gamma U & (y > 0), \\ 0 & (y < 0). \end{cases}$$

The momentum equations have been augmented by the drag in the form of Chézy formula [44, 2] $-\gamma u f(|\boldsymbol{u}|)$, with the empirical estimate of the coefficient γ, which takes account the turbulent boundary layer. We take $f(|\boldsymbol{u}|) = |\boldsymbol{u}|$ as been used in hydraulic practice over a century. We consider, as an unperturbed state, a tangential velocity discontinuity lying along the x-axis, namely, a uniform velocity U in the half plane $(y > 0)$ and no flow in the rest $(y < 0)$. We assume that, in the unperturbed state, the fluid layers on the both sides have the same depth H.

Disturbances, of infinitesimal amplitude, $(\tilde{u}, \tilde{v})$ in the velocity field and $\tilde{h}$ in the height of the free surface, are superimposed as

$$\begin{aligned} &u(x, y, t) = U_0 + \tilde{u}(x, y, t), v(x, y, t) = \tilde{v}(x, y, t), \\ &h(x, y, t) = H + \tilde{h}(x, y, t), \end{aligned} \tag{3.2}$$

The linearized form of the shallow-water equations (3.1) for the disturbance reads

$$\begin{aligned} &D_0\tilde{h} + H(\tilde{u}_x + \tilde{v}_y) = 0, \\ &D_0\tilde{u} + g\tilde{h}_x = -2\gamma U_0\tilde{u}, \\ &D_0\tilde{v} + g\tilde{h}_y = -\gamma U_0\tilde{v}, \end{aligned} \tag{3.3}$$

where

$$D_0 = \frac{\partial}{\partial t} + U_0\frac{\partial}{\partial x},$$

and $U_0 = U$ for $y > 0$ and $U_0 = 0$ for $y < 0$. It is observed that no drag perturbation exerts in the region $(y < 0)$, because of $U_0 = 0$.

We seek the solution in form $e^{i(qx-\omega t)}e^{Ky}$ with real constant q the wavenumber in the streamwise direction and constant K corresponding to the inverse of the decay length in the y direction and ω the frequency, taking complex values. In case a solution with its imaginary part $\mathrm{Im}[\omega] > 0$ is admitted, the basic state is linearly unstable. With this form, (3.3) yields

$$\begin{pmatrix} -i\Omega & -iHq & HK \\ iqg & -i\Omega + 2\gamma U & 0 \\ gK & 0 & -i\Omega + \gamma U \end{pmatrix} \begin{pmatrix} \tilde{h} \\ \tilde{u} \\ \tilde{v} \end{pmatrix} = 0, \tag{3.4}$$

where $\Omega = \omega - qU$. In order for a nontrivial solution $(\tilde{h}, \tilde{u}, \tilde{v}) \neq 0$ to exist, the determinant of the matrix in (3.4) must vanish, supplying the dispersion relation

$$(\Omega + i\gamma U)(\Omega^2 + 2i\gamma U\Omega - c^2q^2) + c^2K^2(\Omega + 2i\gamma U) = 0. \tag{3.5}$$

Writing the relevant root of (3.5) as $K = -K_1$ for $y > 0$ and $K = K_2$ for $y < 0$, with $K_1 > 0$ and $K_2 > 0$, their squared ratio is found to be

$$\frac{{K_1}^2}{{K_2}^2} = \frac{(\omega - qU + i\gamma U)[(\omega - qU)^2 - c^2q^2 + 2i\gamma U(\omega - qU)]}{(\omega - qU + 2i\gamma U)(\omega^2 - q^2c^2)}. \tag{3.6}$$

The boundary conditions to be imposed at the interface are the following. First, the velocity component of the fluid normal to the discontinuity surface is equal on the both sides of the surface and is equal to the velocity of the surface movement in that direction. This kinematical condition is represented as

$$\frac{\partial \zeta}{\partial t} + U\frac{\partial \zeta}{\partial x} = \tilde{v} \quad \text{on } y = \zeta, \tag{3.7}$$

where $y = \zeta(x,t) = ae^{i(qx-\omega t)}$, of infinitesimal amplitude a, is the position of the velocity-discontinuity surface in the horizontal plane. For the normal mode, (3.7) leads to $\tilde{v} = -i\Omega\tilde{\zeta}$. Combining with the last of (3.3), the horizontal displacement $\tilde{\zeta}$ of the interface is connected with the vertical one $\tilde{h}$ via

$$gK\tilde{h} = (\Omega^2 + i\gamma U\Omega)\zeta \quad \text{on } y = \zeta. \tag{3.8}$$

Second, the pressure should be continuous across the discontinuity surface. In the hydrostatic approximation, the pressure perturbation is $\tilde{p} = \rho g\tilde{h}$, and this dynamical boundary condition is reduced to that of the continuity of the wave height across the interface:

$$\tilde{h}_{y=\zeta_1} = \tilde{h}_{y=\zeta_2}, \tag{3.9}$$

where $\tilde{\zeta_{1,2}}$ designates the right- and the left-limit to the interface, respectively. Imposing this condition on (3.8), we obtain

$$\frac{K_1}{K_2} = -\frac{(\omega - qU)^2 + i\gamma U(\omega - qU)}{\omega^2}. \tag{3.10}$$

By combining (3.10) with (3.6), we arrive at the desired dispersion relation between the wavenumber q and the complex frequency ω.

$$\begin{aligned}(\omega - qU + i\gamma U)\Big\{&\omega^4[(\omega - qU)^2 - c^2q^2 + 2iU\gamma(\omega - qU)] \\ &- (\omega - qU)^2(\omega^2 - q^2c^2)(\omega - qU + \gamma Ui)(\omega - qU + 2\gamma Ui)\Big\} = 0.\end{aligned} \tag{3.11}$$

We can easily see that $\omega_1 = qU - i\gamma U$ is a root of (3.11). This root does not contribute to the instability of the interface of tangential velocity discontinuity, since its imaginary part is negative, and is no longer considered. The remaining polynomial is 5th order, as the ω^6 terms are cancelled in the second factor. In order to determine the stability criterion, we have to examine the non-trivial five roots of (3.11). If the imaginary parts of the roots are all non-positive, the discontinuity surface is linearly stable, otherwise the instability is invited.

3.2 Case of no friction

Before looking into the effect of the bottom drag, we review the case of its absence. In case $\gamma = 0$, (3.11) becomes, if the first factor is left out,

$$\left(\omega - \frac{qU}{2}\right)[\omega^2(\omega - qU)^2 + q^3c^2U(2\omega - qU)] = 0, \tag{3.12}$$

manifesting a fifth-order polynomial equation. Its roots ω^0 are written out explicitly as

$$\omega_2^0 = \frac{qU}{2}, \tag{3.13}$$

$$\omega_{\pm\pm}^0 = \frac{q}{2}\left\{U \pm \sqrt{U^2 + 4c^2 \pm 4c\sqrt{U^2 + c^2}}\right\}, \tag{3.14}$$

where the double signs in the suffix correspond to the signs, in the same order, on the right-hand side. The interface of the tangential discontinuity is stable if $U^2 + 4c^2 \pm 4c\sqrt{U^2 + c^2} \geq 0$, or $U \geq \sqrt{8}c$. We have thus recovered the known results of Bezdenkov and Poguste [6, 25]. For $U < \sqrt{8}c$, the imaginary part $\mathrm{Im}[\omega]$ has both positive and negative signs. The mode with $\mathrm{Im}[\omega] > 0$ amplifies exponentially in time t. The instability for $U > \sqrt{8}c$ shares common property with the phenomenon of over-reflection.[28, 32, 1]. Notably, the growth rate is proportional to the wavenumber q, which is characteristic of the Kelvin-Helmholtz instability. The shorter the wavelength is, the faster the corresponding wave grows.

3.3 Influence of bottom drag

We are now in a position to call the bottom drag into play. To gain insight into this frictional effect, we express the root of (3.11) in a power series in a small parameter γ to first order as $\omega = \omega^0 + \gamma\omega^*$. The first term ω^0 corresponds to the solution (3.13) and (3.14) of the dispersion relation with $\gamma = 0$. The second term ω^* is the correction originating from the small bottom drag. The correction to the first root (3.13) is obtained easily by the leading-order of Taylor approximation for small γ as

$$\omega_2^* = -i\frac{U(U^2 - 12c^2)}{4(U^2 - 8c^2)}. \tag{3.15}$$

Hereafter we introduce the Froude number $M = U/c$, the counterpart of the Mach number for the shallow-water flow. With γ, U and c all positive, the condition $\mathrm{Im}[\omega_2^*] > 0$ is $\sqrt{8} < M < \sqrt{12}$ as shown in Fig. 1. The corrections to the remaining four roots (3.14) are manipulated as

$$\begin{aligned}\omega_{\pm-}^* = &\frac{i}{4}\sqrt{c^2 + U^2}\left\{\mp\frac{(c^2 + 4U^2)c - (c^2 + 2U^2)\sqrt{c^2 + U^2}}{\sqrt{4c^2 + U^2 - 4c\sqrt{c^2 + U^2}}}\right.\\ &\left. + U\frac{(9c^2 + 8U^2)c - (9c^2 + 2U^2)\sqrt{c^2 + U^2}}{4c^2 + U^2 - 4c\sqrt{c^2 + U^2}}\right\},\end{aligned} \tag{3.16}$$

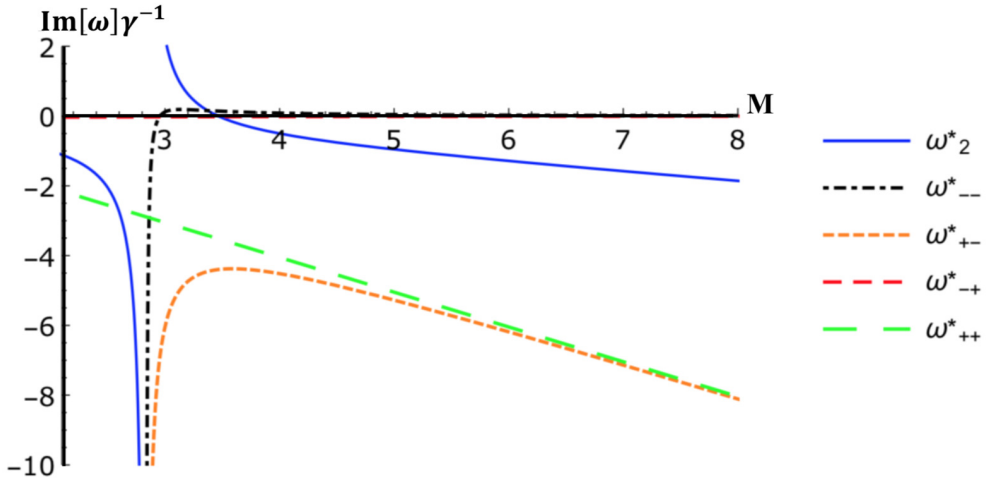

Figure 3.2: The leading-order growth rate $\mathrm{Im}[\omega]/\gamma$ of the displacement of the tangential discontinuity interface for small drag coefficient γ.

$$\omega^*_{\pm+} = \frac{i}{4}\sqrt{c^2+U^2}\left\{\mp\frac{(c^2+4U^2)c+(c^2+2U^2)\sqrt{c^2+U^2}}{\sqrt{4c^2+U^2+4c\sqrt{c^2+U^2}}}\right.$$
$$\left. - U\frac{(9c^2+8U^2)c+(9c^2+2U^2)\sqrt{c^2+U^2}}{4c^2+U^2+4c\sqrt{c^2+U^2}}\right\}. \tag{3.17}$$

In Fig. 3.2, we draw $\mathrm{Im}[\omega^*_2]$ with solid line and $\mathrm{Im}[\omega^*_{\pm+}]$ with different dashed lines as functions of q. At $M=\sqrt{8}$, $\omega^*_{\pm-}$ diverges as is read off from (3.16), and for $M<\sqrt{8}$, $\omega^*_{\pm-}$ becomes real, resulting in $\mathrm{Im}[\omega^*_{\pm-}]=0$. For all values of $M>\sqrt{8}$, $\mathrm{Im}[\omega^*_{+-}]<0$. For $M>\sqrt{9/2+3\sqrt{2}}\approx 2.9568$, $\mathrm{Im}[\omega^*_{--}]>0$ but, for $\sqrt{8}\le M\le\sqrt{9/2+3\sqrt{2}}$, $\mathrm{Im}[\omega^*_{--}]\le 0$. Over the entire range of Fr, $\mathrm{Im}[\omega^*_{++}]<0$, whereas $\mathrm{Im}[\omega^*_{-+}]>0$ for $M<\sqrt{9/2-3\sqrt{2}}\approx 0.50731$ and $\mathrm{Im}[\omega^*_{-+}]\le 0$ for $M\ge\sqrt{9/2-3\sqrt{2}}$.

Notice that the correction terms ω^*_2 and $\omega^*_{\pm\pm}$ of $O(\gamma)$ are all independent of the streamwise wavenumber q, while the leading-order terms (3.13) and (3.14) are linear in q. In the instability regime $M<\sqrt{8}$, the growth rate is dominated by the leading-order term $\mathrm{Im}[\omega^0]$ with large values of q. Therefore we do not any longer consider the frictional effect in this regime, and concentrate on the stability regime $M\ge\sqrt{8}$. We focus our attention only on the growing modes, ones with ω^*_2 and ω^*_{--}, in the region of $M>\sqrt{8}$. The Taylor-series solutions suggest that, when M exceeds $\sqrt{8}\approx 2.8284$, the drag force makes unstable the interface of velocity discontinuity, with the ω_2 mode growing. At $M=\sqrt{9/2+3\sqrt{2}}\approx 2.9568$, the mode with ω_{--} is excited and, as M further increases, it takes over the ω_2 mode. For $M>\sqrt{12}\approx 3.4641$, the ω_{--} mode is solely amplifiable, though the growth rate $\mathrm{Im}[\omega_{--}]$ is small.

The first-order correction terms ω^*_2 and ω^*_{--} diverge at $M=\sqrt{8}$. To carefully treat this seemingly singular behavior, we choose $M=2.83$, and solve numerically the dispersion relation (3.11), with the first factor removed. The real frequency $\mathrm{Re}[\omega]$ and the growth rate $\mathrm{Im}[\omega]$ are displayed as functions of γ in Figs. 3.3 and

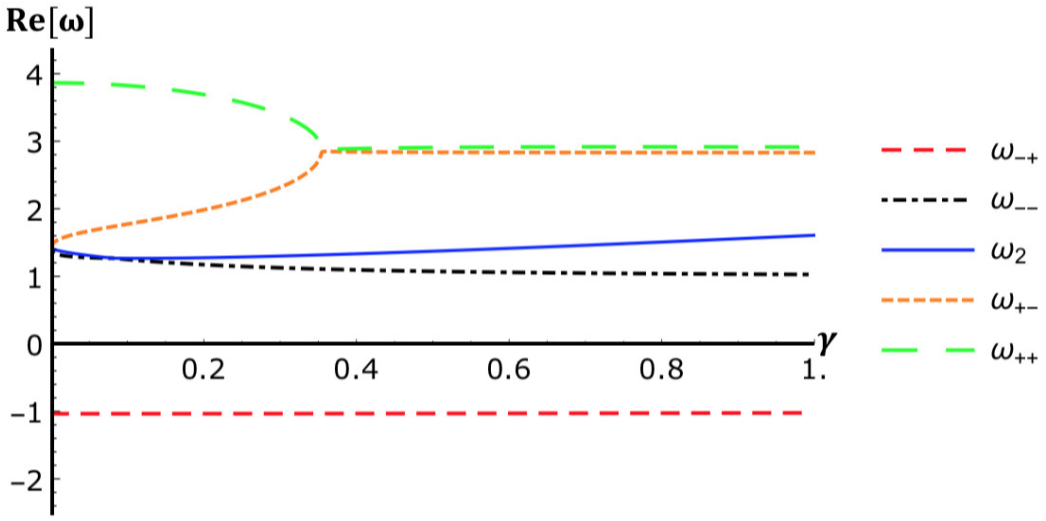

Figure 3.3: The real part Re[ω] of numerical solution of the dispersion equation (3.11) is a function of γ for $M = 2.83$ and $0 \leq \gamma \leq 1$.

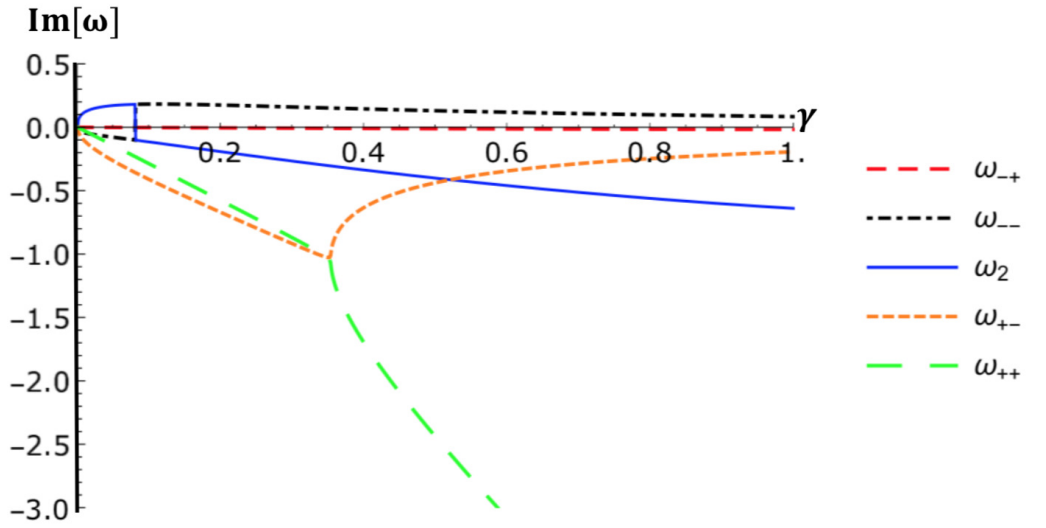

Figure 3.4: The imaginary part Im[ω] of numerical solution of the dispersion equation (3.11) is a function of γ for $M = 2.83$ and $0 \leq \gamma \leq 1$.

3.4 respectively, with solid line for ω_2 and different dashed lines for $\omega_{\pm\pm}$.

We detect the abrupt alteration of the curves of Im[ω_2] and Im[ω_{--}] at the value of γ where their real parts, Re[ω_2] and Re[ω_{--}], approach closest to each other. For values of M close to $\sqrt{8}$, this transition looks abrupt. For $M = 3$, a value less close to $\sqrt{8}$, the alteration of the growth rate occurs moderately and is convincingly recognized as shown by Fig. 3.5, in which the both real and the imaginary parts of ω_2 and ω_{--} are simultaneously drawn. Figure 3.4 illustrates that only the mode with ω_2 prevails as far as γ is small, but that, as γ is increased, it is abruptly superseded by the mode with ω_{--} at $\gamma \approx 0.0815$. The latter is the

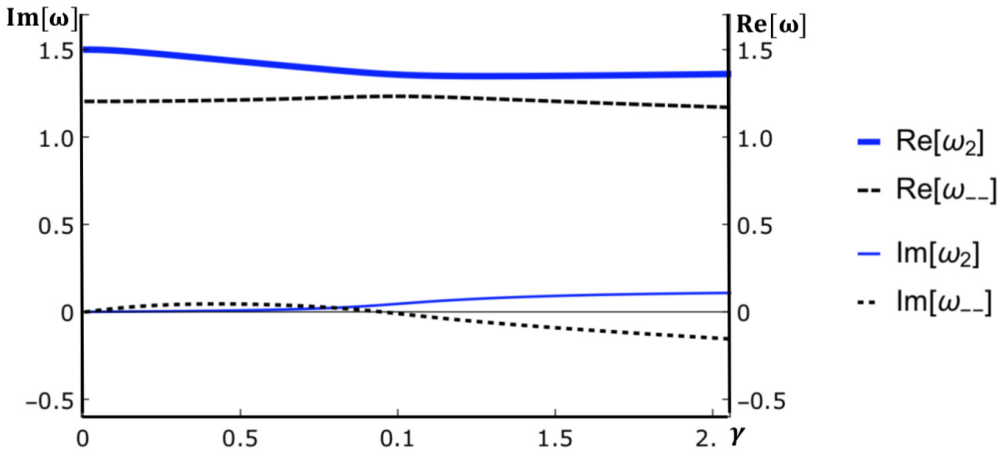

Figure 3.5: Numerical solutions of dispersion equation (3.11) for wave frequency ω. Imaginary parts and Real parts of ω_2, ω_{--} displayed simultaneously, for $M = 3.0$.

sole instability mode in its range of larger values. For $M = 2.83$, the instability of the interface of discontinuity in tangential velocity, with its origin lying in the effect of the bottom drag, takes place for all values of M greater than $\sqrt{8}$, though growth rate decreases with γ for its large values. The growth rate itself remains rather small, and the divergence of ω_2^* and $\omega_{\pm-}^*$ at $M = \sqrt{8}$, as seen in (3.15) and (3.16), implies simply that these are not expressible in the form of power series in γ around $\gamma = 0$ for $M = \sqrt{8}$. We have repeated numerical calculation of the growth rate of instability $\mathrm{Im}[\omega]$ for various values of M over a wide range of γ. There is always at least one of the roots ω with the positive imaginary part which induces to the amplification of wave. Therefore, the interface is always destabilized. In other words, the instability occurs for the entire range of the drag coefficient $\gamma(> 0)$. The asymptotics of the five roots of (3.11), at large values of γ, are manipulated with ease as

$$\omega_2 = qU - 2i\gamma U, \tag{3.18}$$

$$\omega_{\pm+} = qU - iq^2U\frac{U^2 \pm \sqrt{(U^2-c^2)^2+c^4}}{2\gamma(U^2-c^2)}, \tag{3.19}$$

$$\omega_{\pm-} = \pm\left\{qc - \frac{iq^2c^3}{2\gamma U(U \mp c)}\left[1 - \frac{2iq(U \mp c)}{\gamma U}\right]\right\}, \tag{3.20}$$

In the above, $Im[\omega_{--}] > 0$ signifies that the dissipation induced instability is never suppressed for large values of the drag coefficient. We are thus led to a conclusion that, in the presence of the drag of the Chézy type, there is no range of M for stabilization.

3.4 Discusion

We have investigated the effect of bottom friction on the linear stability of interface in a tangential-velocity discontinuity in a shallow water. The stability condition

$M \geq \sqrt{8}$ for the case of no bottom drag [6] is recovered. The bottom friction drastically changes this result, and the interface is destabilized over entire range of the Froude number $M = U/c$, irrespective of the drag strength.

Our result provides an example of the dissipation-induced instabilities that are ubiquitous in nature. This category of instability is usually considered for a small amount of dissipation. The instability persists in the regime of strong dissipation. We have obtained an unusual result that the instability mode is excited even for a large amount of dissipation; the discontinuity interface is linearly unstable over the entire range of drag coefficient as opposed to other models. In a closely related problem of a shear flow [44], only the effect of a small drag force was addressed.

The instability of tangential discontinuity interface has bearing with the over-reflection [1, 37, 44]. The frictional effect on the latter is worth pursuing. All these questions, particularly the Hamiltonian mechanical viewpoint, invite a future study.

4. Stability of a layer of simple shear flow bounded by layers of uniform flows in shallow water

Early treatments of KHI usually assumed the profile of shear velocity to be zero of thickness (i.e. the vortex sheet approximation) as considered by Landau (1944) [24] and other authors. However, in reality, such "discontinuities" in velocity have a finite thickness L, the effects of which becomes significant if the instability wave length $\lambda < L$. Michalke (1964) [27] considered the effects of a hyperbolic tangent profile of shear velocity on Kelvin Helmholtz Instability in an incompressible fluid. He found that a velocity transition stabilizes flow for all wavelengths shorter than the width of the shear layer. Blumen *et al.* (1975) [7] examined the hyperbolic tangent profile in a compressible fluid. They showed that instability occurs at all Mach numbers. The linear profile was treated by Chandrasekhar (1961) [9], Vallis (2005) [38] and others for an incompressible fluid. These authors found results which are similar to those found in the hyperbolic tangent case considered by Michalke.

The linear shear flow of bounded or unbounded extent in shallow water of constant depth was investigated numerically by Satomura (1981) [34] and by Takehiro and Hayashi (1992) [37]. The latter authors also considered reflection by the flow and showed that over-reflection occurred. Both of these investigations were based upon numerical solution of the governing ordinary differential equation.

Here, we consider the effect of a linear-shear layer of finite thickness on the stability characteristics of the zero-thickness mode in a shallow water flow. The simple shear, with the flow velocity as a linear function of the normal coordinate, is assumed in the middle layer as shown in Figure 4.1. In the simple shear (region I), the combination of linearized equations of motion and continuity equation takes the form of Whittaker equation. The dispersion relation of wave frequency and other characteristics of wave is found to involve the Whittaker functions and their first derivatives. We confirm that the appropriate limits of these functions are reduced to various known cases.

In previous chapters, we showed that the interface of tangential velocity discontinuity with a zero thickness layer is stabilized for large Froude number. In the case $L \to 0$, by taking an approximation of Whittaker functions, this result is recovered in subsection 4.2.1. The shear layer of finite thickness totally alters the stability characteristics of the zero-thickness model. The simple shear flow in an incompressible fluid given by Vallis [38] is well known stable for the short wavelength approximation but unstable for the long wave-length approximation. This result is confirmed in subsection 4.2.2 by taking limit of Whittaker functions for gravity-wave velocity $c \to \infty$. In section 4.3, we analysis the instability of the sim-

ple shear flow in a shallow water numerically. Thereafter, we show that the simple layer flow of finite thickness is linearly unstable for the entire range of the Froude number. The last section (section 4.4) gives a brief summary and discussions of this chapter.

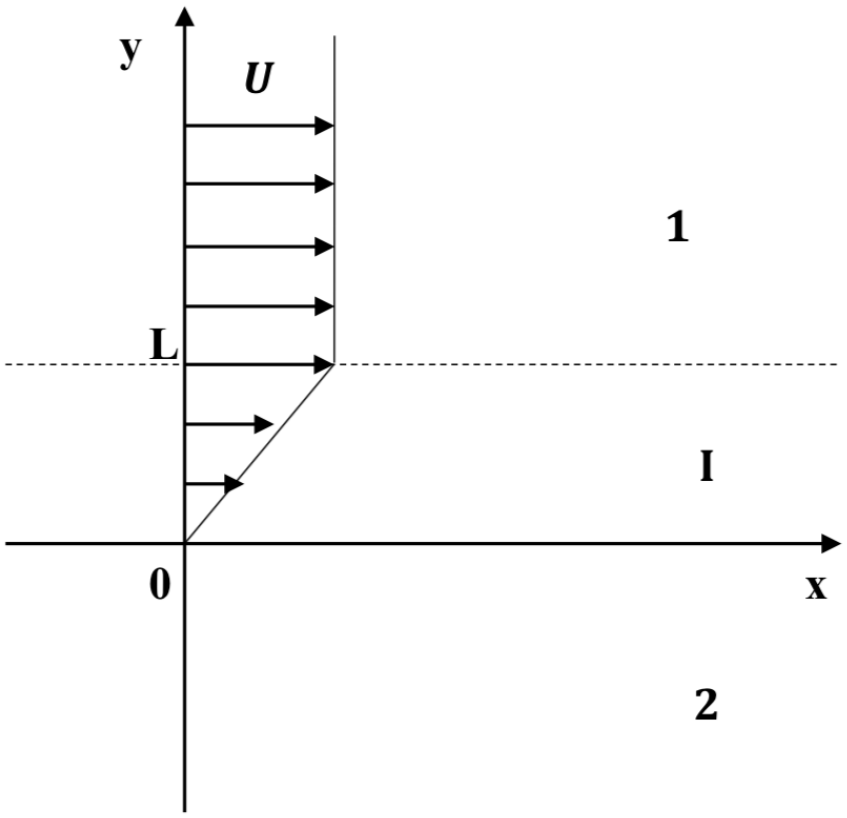

Figure 4.1: Geometry and coordinate system for a simple shear layer in a shallow water flow. Region 1 ($y > L$) is considered that fluid is moving with uniform velocity U in the $x-$ direction. Region I ($0 < y < L$) contains the linear velocity $U = U/Ly$, and region 2 has no flow.

4.1 Derivation of Dispersion equation

We begin this section by deriving the stability equations for infinitesimal perturbation in a shallow water flow. The flow geometry is assumed to have the depth H. Let $U = U(y)$ be the base flow, i.e., the flow lies along the $x-$ axis that varies in the $y-$ direction. The fluid can be divided into three regions (see Figure 4.1). Let us consider the disturbances, of infinitesimal amplitude, $(\tilde{u}, \tilde{v})$ in the velocity field and $\tilde{h}$ in the height of the free surface as follow

$$\begin{aligned} &u(x,y,t) = U(y) + \tilde{u}(x,y,t), v(x,y,t) = \tilde{v}(x,y,t), \\ &h(x,y,t) = H + \tilde{h}(x,y,t), \end{aligned} \tag{4.1}$$

where,

$$U(y) = \begin{cases} U = \text{constant} & y \geq L \text{ region 1}, \\ \frac{U}{L} y & 0 < y < L \text{ region I}, \\ 0 & y < 0 \text{ region 2}. \end{cases} \tag{4.2}$$

We consider all perturbation quantities to vary as $e^{i(qx-\omega t)}$, for a given y, where q is the real wave number in the $x-$ direction and ω is the wave frequency. The linearized equations of motion and continuity equation for wave perturbation yield

$$\begin{aligned} &\frac{D\tilde{h}}{Dt} + H(\tilde{u}_x + \tilde{v}_y) = 0, \\ &\frac{D\tilde{u}}{Dt} + \tilde{v}\frac{\partial U}{\partial y} + g\tilde{h}_x = 0, \\ &\frac{D\tilde{v}}{Dt} + g\tilde{h}_y = 0, \end{aligned} \tag{4.3}$$

in which

$$\frac{D}{Dt} = \frac{\partial}{\partial t} + U(y)\frac{\partial}{\partial x}. \tag{4.4}$$

The first equation of (4.3) is the mass conservation equation, the two last equations are the momentum equations.

Taking derivative of the two last equations (4.3) on x and y, respectively

$$, yields \frac{D}{Dt}\left(\frac{\partial \tilde{u}}{\partial x} + \frac{\partial \tilde{v}}{\partial y}\right) + 2\frac{\partial \tilde{v}}{\partial x}\frac{\partial U}{\partial y} + g\left(\frac{\partial^2}{\partial x^2} + \frac{\partial^2}{\partial y^2}\right)\tilde{h} = 0 \tag{4.5}$$

Substituting the first equation of (4.3) into equation (4.5), we have

$$\frac{D^2\tilde{h}}{Dt^2} - 2H\frac{\partial \tilde{v}}{\partial x}\frac{\partial U}{\partial y} - gH\left(\frac{\partial^2}{\partial x^2} + \frac{\partial^2}{\partial y^2}\right)\tilde{h} = 0 \tag{4.6}$$

Taking derivative of the last equation of (4.3) on x to reduce

$$\frac{\partial \tilde{v}}{\partial x} = \frac{qg}{\omega - qU}\frac{\partial h}{\partial y}, \tag{4.7}$$

and then substituting into equation (4.6), we obtain

$$\frac{D^2\tilde{h}}{Dt^2} - 2\frac{qgH}{\omega - qU}\frac{\partial \tilde{h}}{\partial y}\frac{\partial U}{\partial y} - gH\left(\frac{\partial^2}{\partial x^2} + \frac{\partial^2}{\partial y^2}\right)\tilde{h} = 0. \tag{4.8}$$

Simplify this equation gives

$$\begin{aligned} &\frac{D^2\tilde{h}}{Dt^2} - 2\frac{qc^2}{\omega - qU(y)}\frac{\partial\tilde{h}}{\partial y}\frac{\partial U}{\partial y} - c^2\left(\frac{\partial^2}{\partial x^2} + \frac{\partial^2}{\partial y^2}\right)\tilde{h} = 0, \\ \Longleftrightarrow\ &\frac{\partial^2\tilde{h}}{\partial y^2} + 2\frac{q}{\omega - qU(y)}\frac{\partial\tilde{h}}{\partial y}\frac{\partial U}{\partial y} + \left[\frac{\left[\omega - qU(y)\right]^2}{c^2} - q^2\right]\tilde{h} = 0, \end{aligned} \tag{4.9}$$

where $c = \sqrt{gH}$ is the velocity of gravity wave.

In the region 1 $(y > L)$, the basic flow $U(y) = U$ is a constant then equation (4.9) takes the simple form

$$\frac{\partial^2\tilde{h}_1}{\partial y^2} + \left[\frac{\left[\omega - qU(y)\right]^2}{c^2} - q^2\right]\tilde{h}_1 = 0, \tag{4.10}$$

which has solution in the following form

$$\tilde{h}_1 = A_1 e^{i(qx-\omega t)}e^{-K_1 y}, \tag{4.11}$$

in which A_1 is an arbitrary constant. We obtain easily relation between wave number K_1 in $y-$ direction and other characteristics of wave as follows

$$K_1^2 = q^2 - \frac{(\omega - qU)^2}{c^2}. \tag{4.12}$$

Similarly in the region 2 $(y < 0)$, we have $U(y) = 0$ equation (4.9) gives solution

$$\tilde{h}_2 = A_2 e^{i(qx-\omega t)}e^{K_2 y}, \tag{4.13}$$

in which A_2 is an arbitrary constant. Then we obtain

$$K_2^2 = q^2 - \frac{\omega^2}{c^2}. \tag{4.14}$$

In the region I, $U(y) = Uy/L$ and we transform variables to dimensionless variables

$$M = \frac{U}{c},\ \hat{q} = qL,\ \hat{\omega} = \frac{\omega}{qc},\ \hat{y} = \frac{M}{L}y - \hat{\omega}, \tag{4.15}$$

then equation 4.6 transforms to

$$\frac{\partial^2\tilde{h}_I}{\partial\hat{y}^2} - \frac{2}{\hat{y}}\frac{\partial\tilde{h}_I}{\partial\hat{y}} + \left[\frac{\hat{q}^2}{M^2}\left(\hat{y}^2 - 1\right)\right]\tilde{h}_I = 0. \tag{4.16}$$

We set $Y = \alpha\hat{y}^2$ and $\tilde{h}(\hat{y}) = \hat{y}W(\hat{y})$, the above equation yields

$$\frac{\partial^2 W}{\partial Y^2} + \left[-\frac{1}{2Y^2} + \frac{\hat{q}^2}{M^2}\left(\frac{1}{4\alpha^2} - \frac{1}{4\alpha Y}\right)\right]W = 0. \tag{4.17}$$

If we assume that

$$4\tau = \frac{\hat{q}}{M},\ \alpha = i4\tau,\ m = \frac{\sqrt{3}}{2},\ \kappa = i\tau, \tag{4.18}$$

then equation (4.16) is reduced in the form of Whittaker equation,

$$\frac{\partial^2 W}{\partial Y^2} + \left[-\frac{1}{4} + \frac{\kappa}{Y} + \frac{1/4 - m^2}{Y^2}\right] W = 0. \tag{4.19}$$

In other words, in the region I ($0 < y < L$), equation (4.9) is reducible to the form of Whittaker equation of two parameters κ, m and an argument Y (see Whittaker and Watson, 1950 [43]); the basic solutions to (4.19) are given by

$$M_{\kappa,\pm m}(Y) = Y^{1/2\pm m} e^{-Y/2}\left[1 + \frac{\frac{1}{2} \pm m - \kappa}{1!(1 \pm 2m)} Y + \frac{(\frac{1}{2} \pm m - \kappa)(\frac{3}{2} \pm m - \kappa)}{2!(1 \pm 2m)(2 \pm 2m)} Y^2 + ...\right]. \tag{4.20}$$

General solution of equation (4.19) is written in the form [43]:

$$W(Y) = B_1 M_{\kappa,m}(Y) + B_2 M_{\kappa,-m}(Y), \tag{4.21}$$

where B_1, B_2 are arbitrary constants and $Y = 4i\tau\hat{y}^2 = 4i\tau\left(\frac{M}{L}y - \hat{\omega}\right)^2$. Therefore, equation (4.16) has solution $\tilde{h}_I$ as follows

$$\tilde{h}_I(y) = \left(\frac{M}{L}y - \hat{\omega}\right)\left[B_1 M_{\kappa,m}\left[\alpha\left(\frac{M}{L}y - \hat{\omega}\right)^2\right] + B_2 M_{\kappa,-m}\left[\alpha\left(\frac{M}{L}y - \hat{\omega}\right)^2\right]\right]. \tag{4.22}$$

We rewrite equations (4.12), (4.14) using dimensionless variables as follows

$$\begin{aligned} K_1^2 &= \frac{\hat{q}^2}{L^2}\left[1 - (\hat{\omega} - M)^2\right], \\ K_2^2 &= \frac{\hat{q}^2}{L^2}\left[1 - \hat{\omega}^2\right]. \end{aligned} \tag{4.23}$$

The normal components of the velocities at the interfaces should be continuous. Since the displacement in the $y-$ direction is assumed to be small, thus we have

$$\begin{aligned} \tilde{v}_1 &= \tilde{v}_I \text{ at } y \approx L, \\ \tilde{v}_2 &= \tilde{v}_I \text{ at } y \approx 0. \end{aligned} \tag{4.24}$$

Using equation (4.7), the above continuity condition of normal velocities reduces to

$$\begin{aligned} \frac{1}{\hat{\omega} - M}\frac{\partial \tilde{h}_1}{\partial y} &= \frac{1}{\hat{\omega} - M/Ly}\frac{\partial \tilde{h}_I}{\partial y} \text{ at } y = L, \\ \frac{1}{\hat{\omega}}\frac{\partial \tilde{h}_2}{\partial y} &= \frac{1}{\hat{\omega} - M/Ly}\frac{\partial \tilde{h}_I}{\partial y} \text{ at } y = 0. \end{aligned} \tag{4.25}$$

The pressure should be continuous across the interface. In the hydrostatic approximation, the pressure perturbation $\tilde{p}$ is equal $-\rho g\tilde{h}$. This dynamical boundary condition is reduced to that of the continuity of the wave height across the interfaces, i.e.,

$$\begin{aligned} \tilde{h}_1 &= h_I \text{ at } y \approx L, \\ \tilde{h}_2 &= \tilde{h}_I \text{ at } y \approx 0. \end{aligned} \tag{4.26}$$

Substituting the expressions (4.11), (4.13), (4.17) into the boundary conditions (4.25) and (4.26), we obtain the dispersion relation between dimensionless wave frequency $\hat{\omega}$ and other characteristics of wave as follows

$$\begin{aligned}
&\left[\left(\frac{M}{L}+K_1(M-\hat{\omega})\right)M_{\kappa,m}\left(\alpha(M-\hat{\omega})^2\right)+(M-\hat{\omega})M'_{\kappa,m}\left(\alpha(M-\hat{\omega})^2\right)\right]\times \\
&\qquad\left[\left(\frac{M}{L}+K_2\hat{\omega}\right)M_{\kappa,-m}\left(\alpha\hat{\omega}^2\right)-\hat{\omega}M'_{\kappa,-m}\left(\alpha\hat{\omega}^2\right)\right]- \\
&\left[\left(\frac{M}{L}+K_1(M-\hat{\omega})\right)M_{\kappa,-m}\left(\alpha(M-\hat{\omega})^2\right)+(M-\hat{\omega})M'_{\kappa,-m}\left(\alpha(M-\hat{\omega})^2\right)\right]\times \\
&\qquad\left[\left(\frac{M}{L}+K_2\hat{\omega}\right)M_{\kappa,m}\left(\alpha\hat{\omega}^2\right)-\hat{\omega}M'_{\kappa,m}\left(\alpha\hat{\omega}^2\right)\right]=0,
\end{aligned} \tag{4.27}$$

in which, $M'_{\kappa,\pm m}$ denote the first derivative of Whittaker function $M_{\kappa,\pm m}$ respectively on y. We recall equation (4.18) here,

$$4\tau=\frac{\hat{q}}{M},\ \alpha=i4\tau,\ m=\frac{\sqrt{3}}{2},\ \kappa=i\tau, \tag{4.28}$$

In case, there exits at least one solution $\hat{\omega}$ of (4.27) with its imaginary part $\mathrm{Im}[\hat{\omega}]>0$, the basis state is linearly unstable. In other words, the simple shear flow is stable if only if all solutions of (4.27) have non-positive imaginary part, otherwise the instability is induced. We note that the signs of K_1, K_2 defined in equation (4.23) should be chosen corresponding to the inverse of the decay length in y direction.

We can see from equation (4.27) that for a given Froude number M, only the changes in $\hat{q}$ has to be considered. Now $\hat{q}=qL$ with q being wave number in $x-$direction and L being the thickness of simple shear.

4.2 Asymptotic approximations of Whittaker functions

In this section, the limiting cases of the solutions of equation (4.19) are considered, which correspond to well-known problems. The asymptotics of Whittaker functions $M_{\kappa,\pm m}(Y)$ are examined depending on two parameters $\kappa=i\tau, m$ the one where an argument $Y=4\tau(M/Ly-\hat{\omega})^2=4\tau\hat{y}^2$. The first case to be discussed is that where $\tau\to 0$, which corresponds to the instability problem without a shear layer as considered by Bedenzkov and Pogutse [6]. Then the limiting case for $c\to\infty$ is for the stability problem of a shear layer in an incompressible fluid as considered by Vallis [38].

The series expressions of Whittaker $M-$ functions without expanding in series the exponential part and using the fact that $M_{i\tau,\pm m}(4i\tau\hat{y}^2)$ are real functions for real τ, m and $\hat{y}$ obtained by both Kuechemann [22] and Graham [40]. One thus after some algebra obtains the following forms

$$M_{i\tau,\pm m}(4i\tau\hat{y}^2)=\hat{y}^{1/2\pm 2m}\left[\mathrm{Cos}(2\tau\hat{y}^2)\sum_{n=0}^{\infty}a_n(4\tau\hat{y}^2)^n+\mathrm{Sin}(2\tau\hat{y}^2)\sum_{n=0}^{\infty}b_n(4\tau\hat{y}^2)^n\right], \tag{4.29}$$

where the coefficients a_n and b_n are given by

$$\begin{bmatrix} a_n \\ b_n \end{bmatrix} = \begin{bmatrix} \tau & -\left(\frac{2n-1}{2} \pm m\right) \\ \left(\frac{2n-1}{2} \pm m\right) & \tau \end{bmatrix} \begin{bmatrix} a_{n-1} \\ b_{n-1} \end{bmatrix}, \tag{4.30}$$

with $m = \sqrt{3}/2$ and $a_0 = 1, b_0 = 0$.

The uniform asymptotic expansions for $M_{\kappa,m}(Y)$ (as well as their derivatives) have been derived by Skovgaard (1966) [35] and Olver (1974) [17]. It should be stressed that one is interested in asymptotic expansions as $\tau \to \infty$ holding uniformly in $\hat{y}$ when $\hat{y}$ ranges over unbounded region as well as asymptotic expansions holding for unbounded τ as $\hat{y} \to \infty$ or 0, i.e., expansions describing the asymptotic behavior of $M_{i\tau,\pm m}(4i\tau\hat{y}^2)$ as function of both τ and $\hat{y}$. The case $\hat{y} \to 0$ or ∞ correspond to incompressible flow or high Froude number limits respectively; the case $\tau \to 0$ or ∞ correspond to the long or short wavelength limits.

4.2.1 Case of the zero thickness layer in a shallow water flow

The case of zero thickness layer is of particular interest since Landau (1944) [24] has shown that one obtains stability of the fluid interface for sufficiently high supersonic tangential velocities. He also remarked that there is an analogy between gravity waves in shallow-water flow of an incompressible fluid and sound waves in a gas two dimensional disturbances. Thereafter, Bezdenkov and Pogutse (1984) [6] considered this kind of stability in a shallow water.

Here, we recover the problem considered by Bezdenkov and Pogutse by approximating Whittaker M-functions for the limit $\tau \to 0$ (or $\hat{q}/M \to 0$) with $\hat{y} = (M/Ly - \hat{\omega})$ finite. The Whittaker functions $M_{i\tau,\pm m}(4\tau\hat{y}^2), \kappa = i\tau$ is limited to the lowest order in τ.

$$\begin{aligned} M_{i\tau,m} &\approx 1 - (4\tau)^2\left(\frac{1}{2}\hat{y}^2 + \frac{1}{4}\hat{y}^4\right) + O(\tau^4), \\ M_{i\tau,-m} &\approx \hat{y}^3 + \frac{1}{2}(4\tau)^2\left(\frac{1}{5}\hat{y}^5 - \frac{1}{14}\hat{y}^7\right) + O(\tau^4). \end{aligned} \tag{4.31}$$

Using these asymptotic expansions, the dispersion equation (4.27) for the leading order of τ takes in the form

$$\begin{aligned} &-(M-\hat{\omega})^2\sqrt{1-(M-\hat{\omega})^2} + \hat{\omega}^2\sqrt{1-\hat{\omega}^2} = 0 \\ \Longleftrightarrow\ &(M-\hat{\omega})^4(1-(M-\hat{\omega})^2) - \hat{\omega}^4(1-\hat{\omega}^2) = 0 \end{aligned} \tag{4.32}$$

This equation gives five solutions as follows

$$\begin{aligned} \hat{\omega}_0^0 &= \frac{M}{2}, \\ \hat{\omega}_{\pm,\pm}^0 &= \frac{M}{2} \pm \frac{1}{2}\sqrt{4 + M^2 - 4\sqrt{M^2+1}}. \end{aligned} \tag{4.33}$$

These solutions coincide with the case considered by Bezdenkov and Pogutse [6] and recovered in the chapter 2. If $4 + M^2 - 4\sqrt{M^2+1} < 0$ reduces two complex conjugate

roots of $\hat{\omega}^0$ so that one with positive imaginary part represents an unstable mode and the other one is a stable mode. Thus, the interface is stable if and only if all roots $\hat{\omega}^0$ are real, in other word if only if Froude number $M \geq \sqrt{8}$.

For asymptotic approximation, we assume that $\hat{\omega} = \hat{\omega}^0 + \tau\tilde{\omega}$, and $\tilde{\omega} \ll 1$, we can obtain $\tilde{\omega}$ from the dispersion equation (4.27) as follows:

$$\tilde{\omega}_{\pm,\pm} = M^3(8+M^2))\times$$
$$[(\hat{\omega}^0 - \frac{M}{2})^2 - 1)\left(6\hat{\omega}^0(\hat{\omega}^0 - \frac{M}{2})^2 - (\hat{\omega}^0 - \frac{M}{2})(M^2 + 14M\hat{\omega}^0 - 8)\right)\sqrt{1-(\hat{\omega}^0 - \frac{M}{2})^2} -$$
$$(\hat{\omega}^0 + \frac{M}{2})^2 - 1)\left(2(-2+M^2)\hat{\omega}^0 - M(2+M^2) + (\hat{\omega}^0 - \frac{M}{2})^2(6\hat{\omega}^0 + 5M)\right)\sqrt{1-(\hat{\omega}^0 + \frac{M}{2})^2}]^{-1}. \tag{4.34}$$

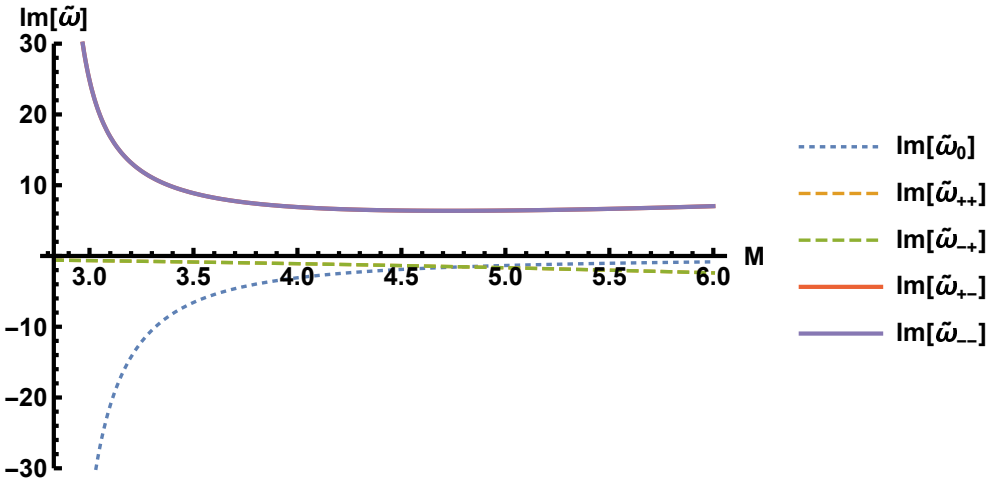

Figure 4.2: The leading-order imaginary parts $\mathrm{Im}[\tilde{\omega}]$ of wave frequency in equation (4.34) varies with Froude number M. Since the conjugate property of roots in (4.34), $\mathrm{Im}[\tilde{\omega}_{+,-}] = \mathrm{Im}[\tilde{\omega}_{-,-}]$ and $\mathrm{Im}[\tilde{\omega}_{+,+}] = \mathrm{Im}[\tilde{\omega}_{-,+}]$. The solid line describes the growth rate of unstable mode, the dashed line and the dotted line show for stable modes.

We see that the solutions $\hat{\omega}_{\pm,-}$ in equation (4.33) have a same imaginary part and $\hat{\omega}_{\pm,+}$ also have a same imaginary part. Therefore, two pairs of graphs of $\mathrm{Im}[\tilde{\omega}_{+,-}]$, $\mathrm{Im}[\tilde{\omega}_{-,-}]$ and $\mathrm{Im}[\tilde{\omega}_{+,+}]$, $\mathrm{Im}[\tilde{\omega}_{-,+}]$ are coincided to each other respectively as shown in Figure 4.2. Here, we choose Froude number $M \geq \sqrt{8}$ when all solutions $\hat{\omega}^0$ in equation (4.33) are real, therefore the imaginary part of $\hat{\omega}$ is proportional to the imaginary part of only $\tilde{\omega}$.

By including a thin simple shear ($\tau \ll 1$ or $qL \ll 1$), the dispersion equation of dimensionless wave-frequency $\hat{\omega}$ always has the complex root with positive imaginary part as depicted in Figure 4.2. In other words, the simple shear flow of finite thickness is linearly unstable for the entire range of the Froude number M. This is contrary to the case of vortex-sheet discontinuity, which is stable for Froude number $M \geq \sqrt{8}$, one may not regard the zero thickness vortex sheet as an adequate

model of a thin simple shear for all relative Frounde numbers of the uniform flows bounding the simple shear layer.

4.2.2 Case of the non-zero thickness layer in an incompressible fluid

The linear profile was considered by Chandrasekhar (1961) [9], Vallis (2005) [38] and others for an incompressible fluid. They showed that the simple shear layer is stable for the short wave-length approximation but unstable for the long wave-length approximation. To consider this case, letting $c \to \infty$ results in $(M/Ly - \hat{\omega}) \to 0$ and $\tau \to \infty$, and $4\tau(M/Ly - \hat{\omega})$ remains finite. The asymptotic expansion of Whittaker function is uniform as $(M/Ly - \hat{\omega})/\tau \to 0$. The expression of Whittaker functions obtain after some straightforward algebra as follows

$$\begin{aligned} M_{\kappa,m} &\approx 4\tau(\frac{M}{L}y - \hat{\omega})\left[\mathrm{Sinh}\left(4\tau(\frac{M}{L}y - \hat{\omega})\right) - \mathrm{Cosh}\left(4\tau(\frac{M}{L}y - \hat{\omega})\right)\right], \\ M_{\kappa,-m} &\approx 4\tau(\frac{M}{L}y - \hat{\omega})\left[\mathrm{Cosh}\left(4\tau(\frac{M}{L}y - \hat{\omega})\right) - \mathrm{Sinh}\left(4\tau(\frac{M}{L}y - \hat{\omega})\right)\right]. \end{aligned} \tag{4.35}$$

Indeed it may be easily verified that the two independent solutions of the stability equation for inviscid incompressible fluctuations in a simple shear flow, i.e., of the equation (4.16) are exactly those given by asymptotic forms in equation (4.35).

Substituting these expression into equation (4.17), then in the dispersion equation (4.27), we obtain

$$\hat{\omega}^2 = \frac{M^2}{4\hat{q}^2}\left[(1-2\hat{q})^2 - e^{-4\hat{q}}\right]. \tag{4.36}$$

These solutions coincide with the one given by Vallis [38]. The flow is stable if $(1-2\hat{q})^2 - e^{-4\hat{q}} \geq 0$. The variation of instability growth rate is depicted in Figure 4.3. The growth rate increases with dimensionless wave number $\hat{q} = qL$ to reach a maximum value, then by increasing $\hat{q}$, the growth rate decreases to zero at $\hat{q} \approx 0.63293$ by solving $(1-2\hat{q})^2 = e^{-4\hat{q}}$. As the wave number goes to zero, the wavelength associated with the disturbances is much larger than the length scale associated with the mean velocity profile. The interface is stabilized for large wave number or a short wavelength approximation, but destabilized for a long wavelength approximation.

The limit of small wave numbers is thus equivalent to the limit of a zero thickness of region I, namely, in the limit $\tau \to 0$ and $\hat{y} \to 0$ the uniform asymptotic of Whittaker functions $M_{i\tau,\pm m}(4\tau\hat{y}^2), \kappa = i\tau$ obtain (see [17]),

$$\begin{aligned} M_{i\tau,m} &\approx 1 - \frac{1}{2}(4\tau\hat{y})^2 + O(\hat{y}^4), \\ M_{i\tau,-m} &\approx \frac{1}{3}(4\tau\hat{y})^3 + \frac{1}{30}(4\tau\hat{y})^5 + O(\hat{y}^7). \end{aligned} \tag{4.37}$$

Substituting these limiting expressions into the dispersion equation (4.27), we keep using the lowest order terms the limit $\hat{y} \to 0$ and $\tau \to 0$. After some straightforward algebra, we obtain

$$(M - \hat{\omega})^2 = -\hat{\omega}^2, \tag{4.38}$$

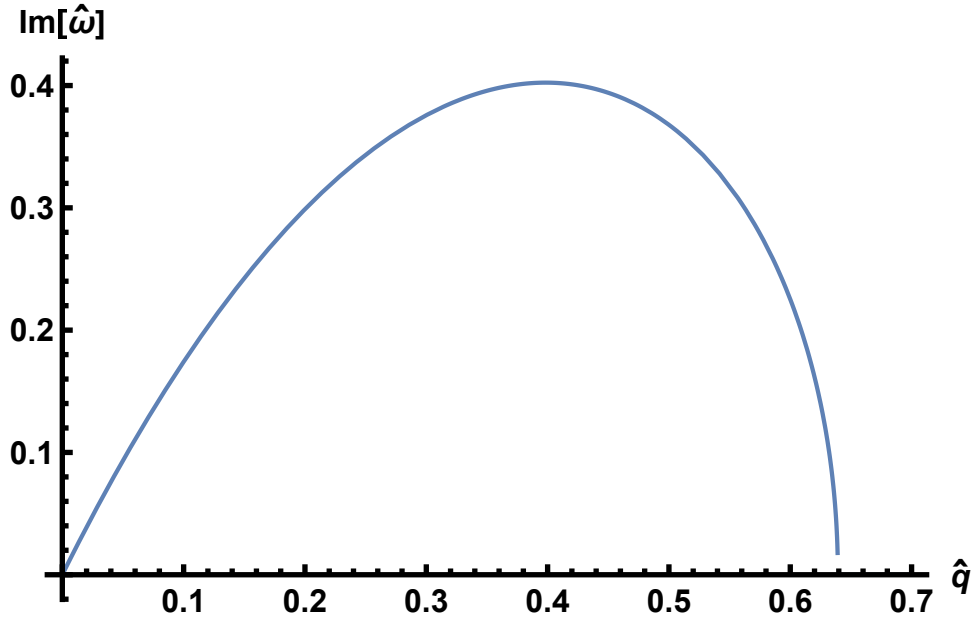

Figure 4.3: Imaginary part of dimensionless wave frequency $\mathrm{Im}[\hat{\omega}]$ proportional to dimensionless wave number $\hat{q} = qL$, and the factor $M^2/4\hat{q}^2$ is taken equal 1. The flow is unstable for $\hat{q} < 0.63293$, with the maximum instability occurring at $\hat{q} \approx 0.39$.

which gives two solutions $\hat{\omega} = \frac{M}{2}(1 \pm i)$ or $\omega = \frac{qU}{2}(1 \pm i)$ as well-known result characterizing the Kelvin-Helmholtz Instability of the incompressible vortex sheet. The interface is unstable even for small different velocity, the growth rate of instability varies linearly with the Froude number M. The growth rate of instability is proportional to the wave number q in $x-$ direction. Therefore, the amplification of waves in the case of the short wavelength (*i.e.* large q) is stronger than in case of the long wavelength (*i.e.* small q).

4.3 Numerical results of stability of the shear layer in a shallow-water flow

Numerical analysis of the stability characteristics with the hyperbolic-tangent velocity profile $U = 0.5(1 + \tanh y)$ in an inviscid homogeneous fluid has been considered by Michalke (1964) [27]. The stability equation was solved by using a Runge-Kutta procedure. This approach was adapted by Blumen(1975) [7] to show that the hyperbolic-tangent shear layer in an compressible fluid is unstable to two dimensional disturbances at each value of the Mach number. This is contrary to the earlier results found for discontinuity of a vortex sheet. They provided a warning against the thoughtless use of vortex sheets, although they have the great advantage of mathematical simplicity.

Because of the analogy between the hydrodynamics of shallow water and polytropic gas dynamics with two dimensional disturbances mentioned by Landau and Lifshitz (1944) [25], we considered the simple shear layer of a shallow water as

shown in section 4.1. It has exact solution related to Whittaker functions. The asymptotic formula for small thickness showed that the simple shear layer is unstable for entire value of Froude number (see subsection 4.2.1). We confirm this result by solving equation (4.27) by using the Mathematica software. The growth of instability mode can be described by considering $\hat{\omega}$ to be complex with q real. Then an imaginary part of $\hat{\omega}$ positive implies a growing mode. It was remarked in section 4.1 that only changes in q and L have to be considered with a given Froude number M. Therefore, we will consider the variation of instability growth rate with a given Froude number M and a given dimensionless wave number $\hat{q} = qL$ respectively.

After taking derivative of Whittaker M-functions with some algebra, equation (4.27) takes the following form

$$
\begin{aligned}
&\Big[-\Big[2M + i\hat{q}(2\hat{\omega}^2 - 1)\Big] M_{\frac{i\hat{q}}{4M},-\frac{\sqrt{3}}{2}}\Big(\frac{i\hat{q}\hat{\omega}^2}{M}\Big) + \Big[2(\sqrt{3}-1)M - i\hat{q}\Big] M_{1+\frac{i\hat{q}}{4M},-\frac{\sqrt{3}}{2}}\Big(\frac{i\hat{q}\hat{\omega}^2}{M}\Big)\Big]\times \\
&\Big[\Big[2iM^2\hat{q} + 2M\Big(1 + \hat{q}\sqrt{1-(M-\hat{\omega})^2} - 2i\hat{q}\hat{\omega}\Big) - \hat{q}\Big(2\hat{\omega}\sqrt{1-(M-\hat{\omega})^2} - i(2\hat{\omega}^2-1)\Big)\Big] \\
&\times M_{\frac{i\hat{q}}{4M},\frac{\sqrt{3}}{2}}\Big(\frac{i\hat{q}(M-\hat{\omega})^2}{M}\Big) + \Big[2(1+\sqrt{3})M + i\hat{q}\Big] M_{1+\frac{i\hat{q}}{4M},\frac{\sqrt{3}}{2}}\Big(\frac{i\hat{q}(M-\hat{\omega})^2}{M}\Big)\Big] \\
&- 2\hat{q}\hat{\omega}\sqrt{1-\hat{\omega}^2}\Big[- M_{\frac{i\hat{q}}{4M},\frac{\sqrt{3}}{2}}\Big(\frac{i\hat{q}\hat{\omega}^2}{M}\Big)\Big(\Big[- 2(-1+\sqrt{3})M + i\hat{q}\Big] M_{1+\frac{i\hat{q}}{4M},-\frac{\sqrt{3}}{2}}\Big(\frac{i\hat{q}(M-\hat{\omega})^2}{M}\Big)\Big) + \\
&\Big[2i\hat{q}M^2 + 2M\Big(1 + \hat{q}\sqrt{1-(M-\hat{\omega})^2} - 2i\hat{q}\hat{\omega}\Big) + \hat{q}\Big(2i\hat{\omega}^2 - 2\hat{\omega}\sqrt{1-(M-\hat{\omega})^2} - i\Big)\Big] M_{\frac{i\hat{q}}{4M},-\frac{\sqrt{3}}{2}}\Big(\frac{i\hat{q}(M-\hat{\omega})^2}{M}\Big) \\
&+ M_{\frac{i\hat{q}}{4M},-\frac{\sqrt{3}}{2}}\Big(\frac{i\hat{q}\hat{\omega}^2}{M}\Big)\Big(\Big[2\hat{q}\sqrt{1-(M-\hat{\omega})^2}(M-\hat{\omega}) + i\Big(2M^2\hat{q} - 2M(i + 2\hat{q}\hat{\omega}) + \hat{q}(-1+2\hat{\omega}^2)\Big)\Big] \\
&\times M_{\frac{i\hat{q}}{4M},\frac{\sqrt{3}}{2}}\Big(\frac{i\hat{q}(M-\hat{\omega})^2}{M}\Big) + \Big[2(1+\sqrt{3})M + i\hat{q}\Big] M_{1+\frac{i\hat{q}}{4M},\frac{\sqrt{3}}{2}}\Big(\frac{i\hat{q}(M-\hat{\omega})^2}{M}\Big)\Big)\Big] \\
&+ \Big[\Big[2iM^2\hat{q} + 2M\Big(1 + \hat{q}\sqrt{1-(M-\hat{\omega})^2} - 2i\hat{q}\hat{\omega}\Big) + \hat{q}\Big(- i - 2\sqrt{1-\hat{\omega}(M-\hat{\omega})^2} + 2i\hat{\omega}^2\Big)\Big] \\
&M_{\frac{i\hat{q}}{4M},-\frac{\sqrt{3}}{2}}\Big(\frac{i\hat{q}(M-\hat{\omega})^2}{M}\Big) + \Big[- 2(-1+\sqrt{3})M + i\hat{q}\Big] M_{1+\frac{i\hat{q}}{4M},-\frac{\sqrt{3}}{2}}\Big(\frac{i\hat{q}(M-\hat{\omega})^2}{M}\Big)\Big]\times \\
&\Big[\Big[2M + i\hat{q}(-1+2\hat{\omega}^2)\Big] M_{\frac{i\hat{q}}{4M},\frac{\sqrt{3}}{2}}\Big(\frac{i\hat{q}\hat{\omega}^2}{M}\Big) + \Big[2(1+\sqrt{3})M + i\hat{q}\Big] M_{1+\frac{i\hat{q}}{4M},-\frac{\sqrt{3}}{2}}\Big(\frac{i\hat{q}\hat{\omega}^2}{M}\Big)\Big] = 0
\end{aligned}
\tag{4.39}
$$

It is more convenient to describe our results graphically by presenting Figures 4.4, 4.5 and explaining them briefly. The solid lines corresponds to the unstable model caused by the instability growing with time. For a given Froude number $M = 3$, Figure 4.4 shows graphs of two imaginary parts $\mathrm{Im}[\hat{\omega}]$ of the frequency wave as a function of the product between wave number q and the thickness layer

L of simple shear. Figure 4.4 shows that the solution of dispersion equation (4.27) appears with at least a pair of complex roots with the same magnitude of imaginary part but opposite signs. In an incompressible fluid, Vallis [38] showed that the simple shear layer is stable for large wave number or short wave limitation. Here, numerically, we show that the simple shear layer in a shallow water flow is unstable for all wave number with a given Froude number.

With a given factor $\hat{q} = qL = 1$, we find one complex root of the dispersion equation (4.27) with positive imaginary part. This root corresponds to the instability model, the growth rate of instability increases with Froude number M as shown in Figure 4.5. This result is contrary to the model of zero thickness where the interface is stable for large Froude number as considered by Bedenzkov and Pogutse [6].

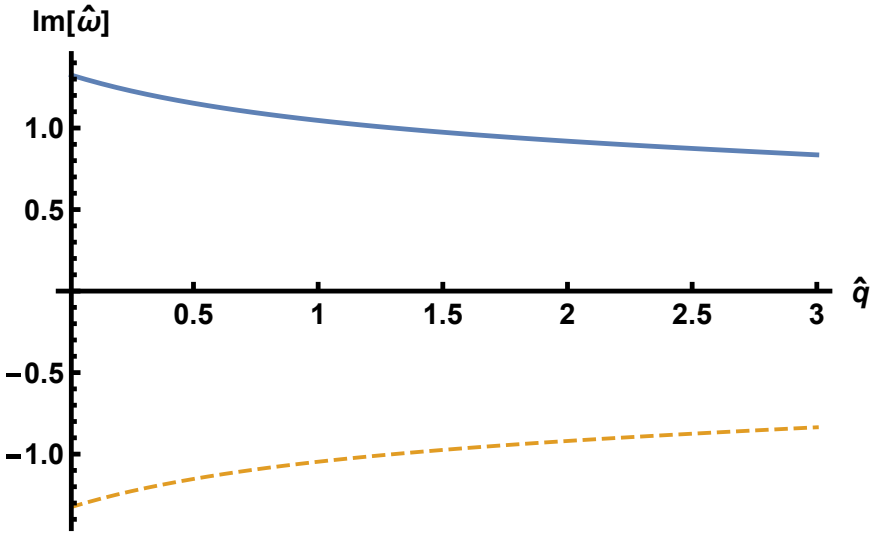

Figure 4.4: Imaginary part Im$[\hat{\omega}]$ varies with the factor $\hat{q} = qL$ for given Froude number $M = 3$. Solid line describes the growth rate of unstable mode with dimensionless wave numbers $\hat{q}$. Dashed line is for a stable mode.

4.4 Discusion

We have discussed the effect of a simple shear layer on the growth of Kelvin Helmholtz instability in a shallow water flow. The simple shear layer is sandwiched between two infinite layers moving parallel with different velocities. The dispersion relation is found to involve the Whittaker functions and their first derivatives. The appropriate asymptotic of Whittaker functions are used corresponding to the various physical conditions to reduce to well known results. Asymptotics of $c \to \infty$ corresponds to the case of an incompressible fluid. The simple shear flow is stable for large wave number or a short wave-length approximation, but unstable for a long wave-length approximation as given by Vallis (2005) [38].

For a vortex sheet approximation (with no simple shear layer), the asymptotics of Whittaker functions for $\tau \to 0$ or $L \to 0$ recovered the instability problem con-

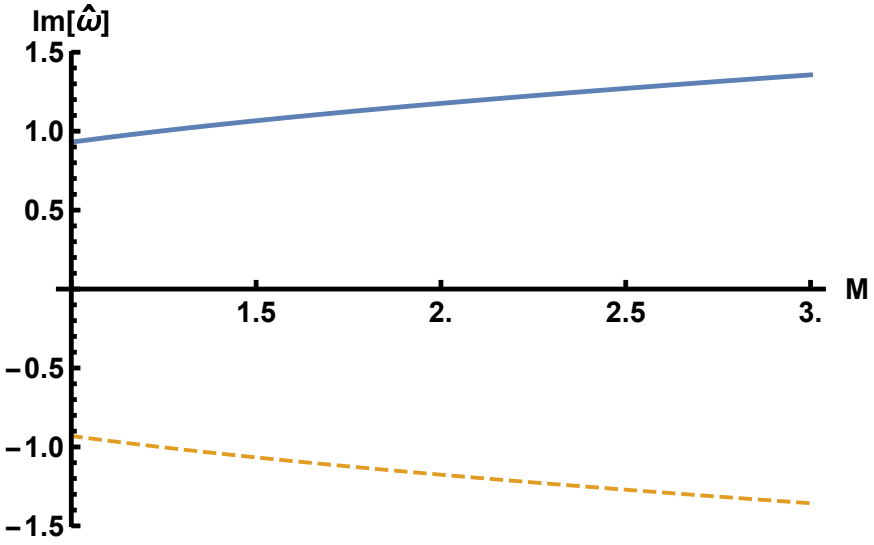

Figure 4.5: Imaginary part $\mathrm{Im}[\hat{\omega}]$ varies with Froude number $M \geq 1$ for given $\hat{q} = qL = 1$. Solid line describes the growth rate of unstable mode with Froude numbers M. Dashed line is for a stable mode.

sidered by Bedenzkov and Pogutse [6]. The interface is stable if Froude number $M \geq \sqrt{8}$. However, by including the thin simple shear, the asymptotic approximation of Whittaker functions for $\tau \ll 1$ or $qL \ll 1$, the dispersion equation of dimensionless wave-frequency $\hat{\omega}$ always has the complex root with positive imaginary part as depicted in Figure 4.2. In other word, the shear layer flow of finite thickness is linearly unstable for the entire range of the Froude number M. This result was confirmed again numerically. Our results are similar in many respects to those presented by Blumen (1975) *et al.* [7] for a hyperbolic tangent profile in a compressible fluid. Thus it is contrary to the zero thickness vortex sheet, which is stable for Froude number $M \geq \sqrt{8}$, one may not regard the zero thickness vortex sheet as an adequate model of a thin simple shear for all relative Froude numbers of the uniform flows bounding the simple shear layer.

5. Conclusion

We have studied the effect of gravity waves on the linear stability of the interface between fluid regions moving parallel with different velocities in the shallow-water flow. Both cases of zero thickness layer (no shear layer at the middle two fluid regions) and non-zero thickness layer (shear layer) were considered. Three problems were investigated in this research, namely, (i) the different gravity waves on the two sides of interface act on the stability; (ii) the effect of frictional bottom on the stability of interface; (iii) the effect of shear layer sandwiched between two infinite layers moving parallel with different velocities on the stability. In section 1.2, we have revisited the linear stability of the interface of a tangential-velocity discontinuity for an incompressible fluid, known as the Kelvin-Helmholtz Instability (KHI) problem. The interface is necessarily unstable, regardless of strength of different velocity. Landau [24] showed that the effect of compressible fluid can suppress KHI and that the interface is stabilized if the velocity difference is equal or greater than $\sqrt{8}$ times sound velocity. This results was recovered in section 1.3. The stability problem of the interface of a tangential-velocity in a shallow water considered by Bezdenkov and Pogutse [6] was revisited in sections 2.2, 3.2, 4.2 to compare with our results in each problem. The stability of a simple layer for an incompressible fluid was examined by Chandrasekhar (1961) [9], Vallis (2005) [38]. They showed that the simple shear layer flow is stable for the short wave-length approximation but unstable for the long wave-length approximation. Their result was visited in subsection 4.2.2.

We first have considered the effect of depth difference on the stability of the interface of a tangential-velocity discontinuity in a shallow water flow. The dispersion relation between wave-frequency and other characteristics of wave is described in the form of a sextic polynomial. Our results show that interface is stabilized if the Froude number $M_1 = U/c_1$ is equal or greater than the critical value M_{1c}. The critical value M_{1c} is a function of the depth ratio $r = H_1/H_2$, also known as ratio of gravity wave velocity c_1 to c_2. The minimum of the critical Froude number $\sqrt{8}$ occurs at $r = 1$, that is, in the same depth case. This coincides with the critical Froude number obtained by Bezdenkov and Pogutse [6]. The sextic polynomial equation of dispersion relation is altered to a quintic polynomial equation in case $r = 1$ and the interface is stabilized if and only if $M_1 \geq \sqrt{8}$. In general cases $r \neq 1$, we find that the critical value M_{1c} is an increasing function with $r > 1$ and a decreasing function for $0 < r < 1$. Both in the case $0 < r < 1$ and the case of $r > 1$, the critical value M_{1c} is always greater than $\sqrt{8}$ as shown in Figure 2.5.

The second problem was made by considering the effect of bottom drag on the interfacial stability of a tangential-velocity discontinuity in a shallow water flow. Without frictional bottom in case of same water-depth [6], the interface is stabilized if the Froude number is equal or greater than the critical value $\sqrt{8}$. The bottom friction drastically changes this result, and the interface is destabilized

over entire range of the Froude number, irrespective of the drag strength. The bottom friction and the internal lateral friction both play significant roles in the linear stability of a two-dimensional shallow-water flow. The analysis is based on the Boussinesq shallow-water equations, this category of instability is usually considered for a small amount of dissipation. We have obtained an unusual result that the instability mode is excited even for a large amount of dissipation; the discontinuity interface is linearly unstable over the entire range of drag coefficient as opposed to other models. Our result provides an example of the dissipation-induced instabilities that are ubiquitous in nature. In a closely related problem of a shear flow [44], only the effect of a small drag force was addressed.

For the last problem, our analysis was made for the linear stability of the shear flow in which the shear layer is sandwiched between two infinite layers moving parallel with different velocities. The velocity profile of shear layer is a linear function of the normal coordinate. The dispersion relation is found to involve the Whittaker functions and their first derivatives. The appropriate limits of these functions correspond to the various physical conditions of problem. For some approximation of Whittaker functions, we recovered well-known results in section 4.2. For a vortex sheet approximation (with no simple shear layer) [6], the interface is stable if Froude number $M \geq \sqrt{8}$. In the incompressible fluid [9, 38], the simple shear flow is stable for large wave number or a short wave-length approximation, but unstable for a long wave-length approximation. Numerically, we find that the simple shear flow changes the stability property of the interface in zero thickness model and leads to the flow being unstable for entire value of Froude number. It is contrary to earlier results found for the discontinuity of a vortex sheet and the simple shear layer in an incompressible fluid. However, this result agrees with the case of hyperbolic tangent profile in a compressible fluid which instability occurs at all Mach numbers considered by Blumen *et al.* (1975) [7].

6. Internship's Report Numerical simulation of an interface between two fluids flowing inside branched pipes

6.1 Problem

A condensate recovery system for an ink jet printer includes an ink reservoir and a condenser. The condenser is in fluid communication with the ink reservoir and is adapted to receive exhaust from the ink reservoir and condense solvent from the exhaust. The condenser includes a fluid inlet for receiving the exhaust from the fluid reservoir, a condensing volume in fluid communication with the inlet, a vent in fluid communication with the condensing volume for venting air from the condenser and a fluid outlet for removing condensed solvent from the condenser and returning the condensed solvent to the ink reservoir. A valve is in fluid communication with the condenser fluid outlet and the fluid reservoir. The valve is operable to open and close to control flow of condensed fluid from the condenser to the fluid reservoir. The motion of fluids in the condenser are two phase flows with exchanging heat between environments through the cooling technology. Therefore, the knowledge of interaction of the interface between two phases helps to design condensers more easily and to improve the cooling system of printers.

In this work, we will simulate the interaction of an interface between two fluids (gas - liquid) flowing inside a T-branched pipe. In case of two-dimension flow is simulated for two phase flow in the plane XZ without the exchange of heat between fluids and environment. The finite element method (FEM) is used to solve a partial differential equation numerically. The software FreeFem++ is used to simulate the phase change of flow. The code is written by the programming language C++. In case of three-dimension flow, we use the commercial software Ansys Fluent version 18.2. The Eulerian multiphase model is used to simulate flow. The heat exchange between fluids and environment of the cooling system of printer is included. The FLUENT solution is based on the following: A single pressure is shared by all phases; Momentum and continuity equations are solved for each phase.

6.2 Numerical simulation

6.2.1 Two dimensions simulation by using FreeFem++ Software

Phase field method - Allen Cahn Equation and Laminar flow (parabolic profile) are used to analyze the two phase flow. The profile across a flat interface in an equilibrium state is written as follows [36]

$$\phi(\epsilon) = \frac{1}{2}\Big[1 + \tanh\Big(\frac{\epsilon}{2\sqrt{\kappa_\phi}}\Big)\Big], \tag{6.1}$$

in which ϵ denotes the signed distance in the direction normal to the interface from the central position, κ_ϕ is the thickness of interface.

Phase field models are usually constructed in order to reproduce a given interface-dynamics. For instance, in solidification problems the front dynamics is given by a diffusion equation for either concentration or temperature in the bulk and some boundary conditions at the interface (a local equilibrium condition and a conservation law), which constitutes the sharp interface model. A number of formulations of the phase field model are based on a free energy function depending on an order parameter (the phase field) and a diffusive field (variational formulations). Equations of the model are then obtained by using general relations of statistical physics. Such a function is constructed from physical considerations, but contains a parameter or combination of parameters related to the interface width. Parameters of the model are then chosen by studying the limit of the model with this width going to zero, in such a way that one can identify this limit with the intended sharp interface model. The finite element method (FEM) is used to solve a partial differential equation numerically. The software FreeFem++ is used to simulate the phase change of flow. FreeFem++ includes a fast interpolation algorithm and a language for the manipulation of data on multiple meshes, in which, the programming was written by C++ language.

The condenser model is given by Table 6.1 and the shape of pipe is shown in Figure 6.1. The initial conditions (at inlet) is given by Table 6.2

Table 6.1: The condenser model of T pipe in 2D

Model	**Length of horizontal branch** L	**High of vertical branch** H	**Diameter** D
2D	$100m$	$100m$	$60mm$

Table 6.2: The initial conditions at inlet.

Averaged velocity u_{in}	**Phase field** ϕ	**Mobility number** M	**Thickness of interphase** κ_ϕ
$0.5\ m/s$	0.3	0.0001	0.00001

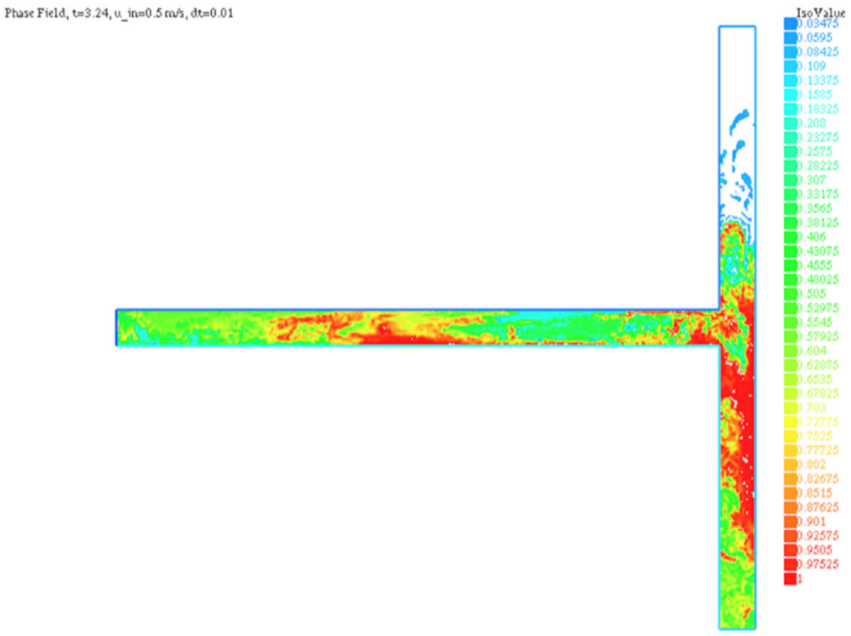

Figure 6.1: Numerical simulation two phase flow in a T-pipe by FreeFem++ at time $t = 3.24$ and time step $dt = 0.01$.

6.2.2 Three dimensions simulation by using Ansys Fluent Software

The Eulerian multiphase model is used to simulate two phase flow in three dimension by using software Ansys Fluent. This model allows for the modeling of multiple separate, yet interacting phases. The phases can be liquids, gases, or solids in nearly any combination. An Eulerian treatment is used for each phase, in contrast to the Eulerian-Lagrangian treatment that is used for the discrete phase model. With the Eulerian multiphase model, the number of secondary phases is limited only by memory requirements and convergence behavior. Any number of secondary phases can be modeled, provided that sufficient memory is available. Volume fraction α_q represents the space occupied between gas phase and liquid phase, and the laws of conservation of mass and momentum are satisfied by each phase individually. The derivation of the conservation equations can be done by ensemble averaging the local instantaneous balance for each of the phases or by using the mixture theory approach.

The volume of phase q, V_q, is defined by

$$V_q = \int_V \alpha_q dV, \tag{6.2}$$

where $\alpha_q = \sum_{q=1}^{n} \alpha_q = 1$.

The internal energy balance for phase q is written in terms of the phase enthalpy

$$H_q = \int c_{p,q} dT_q, \tag{6.3}$$

where $c_{p,q}$ is the specific heat at constant pressure of phase q.

The rate of energy transfer between phases is assumed to be a function of the temperature difference

$$Q_{p,q} = h_{pq}(T_p - T_q), \tag{6.4}$$

where where $h_{pq}(= h_{qp})$ is the heat transfer coefficient between the p^{th} phase and the q^{th} phase, T_p, T_q are the temperature of the p^{th} phase and the q^{th} phase, respectively.

The heat transfer coefficient is related to the p^{th} phase Nusselt number, Nu_p, by

$$h_{pq} = \frac{6\kappa_q \alpha_q (1 - \alpha_q) Nu_p}{d_p^2} \tag{6.5}$$

Here κ_q is the thermal conductivity of the q^{th} phase, $D = (d_p + d_q)/2$ is the average diameter of pipe. The Nusselt number Nu_p is typically determined from one of the many correlations reported in the literature as follows

$$Nu_p = 2.0 + 0.6 Re_p^{1/2} Pr^{1/3}, \tag{6.6}$$

where Re_p is the relative Reynolds number based on the diameter of the p^{th} phase and the relative velocity $|u_p - u_q|$, and Pr is the Prandtl number of the q^{th} phase.

For Eulerian multiphase calculations, Ansys Fluent uses the phase coupled SIMPLE (PC-SIMPLE) algorithm [39] for the pressure-velocity coupling. PC-SIMPLE is an extension of the SIMPLE algorithm [31] to multiphase flows. The velocities are solved coupled by phases, but in a segregated fashion. The block algebraic multigrid scheme used by the density-based solver described in [41] is used to solve a vector equation formed by the velocity components of all phases simultaneously. Then, a pressure correction equation is built based on total volume continuity rather than mass continuity. Pressure and velocities are then corrected so as to satisfy the continuity constraint.

The condenser model is given by Table 6.3 and the shape of pipe is shown in Figure 6.2.

Table 6.3: The condenser model of T pipe in 3D

Model	**Length of horizontal branch** L	**High of vertical branch** H	**Diameter** D
3D	$100m$	$100m$	$6mm$

The initial conditions are given by Table 6.4 at inlet and Table 6.5

Table 6.4: The initial conditions at inlet.

Turbulent intensity	**Turbulent viscosity**	**Mass flow**
0.5%	10	0.01 kg/s

Table 6.5: The initial conditions at outlet.

Turbulent intensity	Turbulent viscosity	Pressure
0.5%	10	Profile Multiplier 1

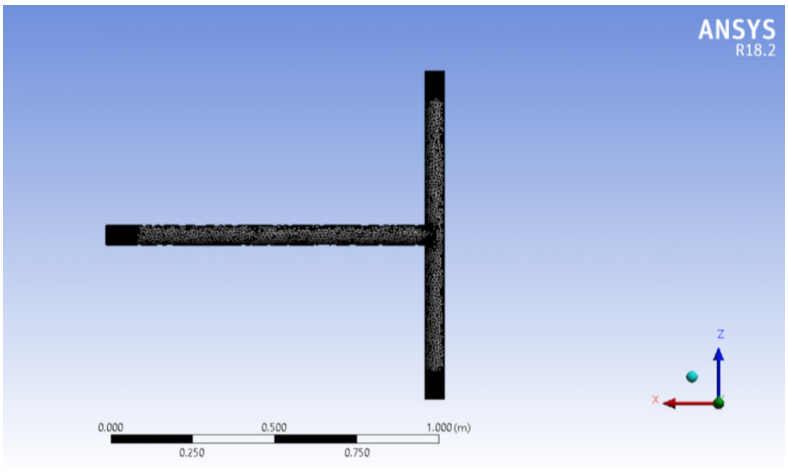

Figure 6.2: 3D Geometry of numerical simulation two phase flow in a branched pipe by Ansys FLuent

6.3 Conclusion

We have simulated two phase flow inside the T-pipe in two dimensions and three dimensions. In case of 2D simulation, the fluids was Nitrogen (gas) and water (liquid). There is no exchange of heat between fluids and environment. In case of 3D simulation, we used the fluids which are using in condenser system of printers Ricoh Technology Center, Ricoh company. In this case, we considered the heat exchange between fluids and environment. The interaction of interface between two fluids depends on the density ratio and the velocity profile of flow. The velocity and pressure of fluids at outlet depends on the shape of interface. The pressure at the bottom outlet is smaller than at the top outlet caused by the effect of the gravity force. The results show the surface tension becomes important related the viscosity of materials and the diameter of pipes. The effect of the surface tension is stronger to a smaller diameter but weaker to a larger diameter. The volume fraction between two phases is calculated through calculating the shape of interface and the transport of heat flux.

The results is restricted as some examples of two phases flow in the T-pipe. The model has not been compared with real models to choose the initial conditions suitable. Because of the security of company, we do not provide the detail information of fluids anymore.

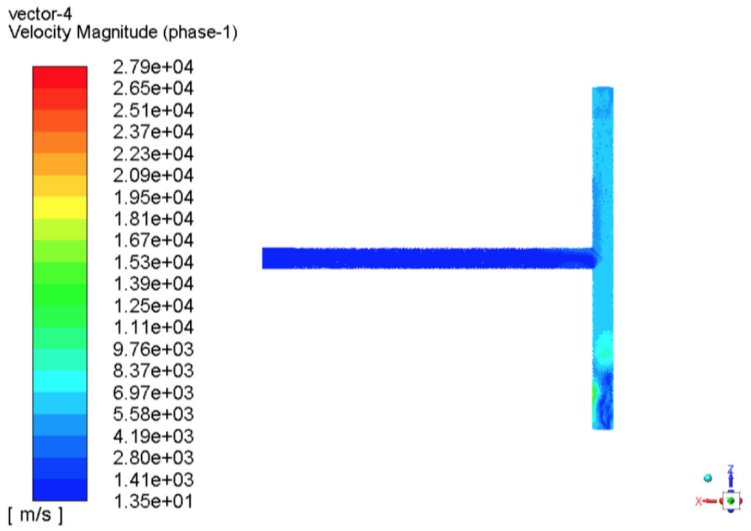

Figure 6.3: Numerical simulation of the velocity of phase 1 (nitrogen) in a T-pipe by Ansys FLuent

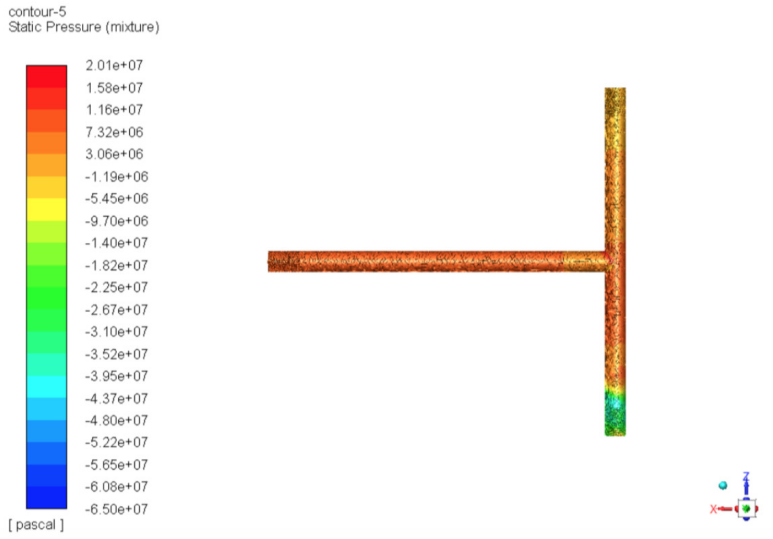

Figure 6.4: Numerical simulation of the pressure in a T-pipe by Ansys FLuent

Acknowledgement

This work was done during three months of the internship program at Ebina Ricoh Technology Center, Ricoh Company in Japan. I would like to thank to Mr. Tomoyasu Hirasawa for being my advisor during the period of the internship program. My sincere thanks also goes to Dr. Ichiro Maeda and all members of Group 2 Loop Heat Pipe (LHP) for supporting me during the working time at Ebina Ricoh Technology Center.

Bibliography

[1] D. J. Acheson, *On over-reflexion*, J. Fluid Mech. **77** (1976), 433–472.

[2] N .J. Balmforth and S. Mandre, *Dynamics of roll waves*, J. Fluid Mech **514** (2004), 1–33.

[3] G. K. Batchelor, *An introduction to fluid dynamics*, Cambridge University Press, 2000.

[4] T. Brooke Benjamin, *Wave formation in laminar flow down an inclined plane*, J. Fluid Mech. **2** (1957), 554–573.

[5] Berlamont and Vanderstappen, *Unstable turbulent flow in open channels*, J. Hydraulic Divison, ASCE **107** (1981), 427–449.

[6] S. V. Bezdenkov and O. P. Pogutse, *Supersonic stabilization of a tangential shear in a thin atmosphere*, Pis'ma Zh. Eksp. Teor. Fiz. **37** (1983), 317–319.

[7] W. Blumen, P. G. Drazin, and D. F. Billings, *Shear layer instability of an inviscid compressible fluid. part 2*, Journal of Fluid Mechanics **71** (1975), no. 2, 305–316.

[8] R. J. Breeding, *A non-linear investigation of critical levels for internal atmospheric gravity waves*, J. Fluid Mech. **50** (1971), 545–563.

[9] Sivaramakrishna Chandrasekhar, *Hydrodynamic and hydromagnetic stability*, 1961.

[10] Paul E. Chang, I-Dee; Russell, *Stability of a liquid layer adjacent to a high-speed gas stream*, Physics of Fluids **8** (1965), 1018–1026.

[11] D. Chen and G. H. Jirka, *Absolute and convective instabilities of plane turbulent wakes in a shallow water layer*, J. Fluid Mech **338** (1997), 157–172.

[12] P. G. Drazin, *Introduction to hydrodynamic stability*, Cambridge Texts in Applied Mathematics, Cambridge University Press, 2002.

[13] I. A. Eltayeb and J. F. McKenzie, *Critical-level behaviour and wave amplification of a gravity wve incident upon a shear layer*, J. Fluid Mech. **72** (1975), 661–671.

[14] J. A. Fejer, *Hydromagnetic reflection and refraction at a fluid velocity discontinuity*, The Physics of Fluids **7** (1963), 499–503.

[15] T. Funada and D. D. Joseph, *Viscous potential flow analysis of kelvin-helmholtz instability in a channel*, J. Fluid Mech. **445** (2001), 263–283.

[16] A. E. Gill, *Instabilities of top-hat jets and wakes in compressible fluids*, The Physics of Fluids **8** (1965), 1428–1430.

[17] Olver F. W. J. and Bullard Edward Crisp, *The asymptotic solution of linear differential equations of the second order for large values of a parameter*, Philosophical Transactions of the Royal Society of London. Series A, Mathematical and Physical Sciences **247** (1954).

[18] Harold Jeffreys, *On the formation of water waves by wind*, Proceedings of The Royal Society A **107** (1925), 189–206.

[19] W. L. Jones, *Reflection and stability of waves in stably stratified fluids with shear flow: a numerical study*, J. Fluid Mech. **34** (1968), 609–624.

[20] J. B. Schnieder Jun Liu and Jerry P. Gollub, *Three-dimensional instabilities of film flows*, Physics of Fluids **7** (1995), 55–67.

[21] R. Krechetnikov and J. E. Marsden, *Dissipation-induced instabilities in finite dimensions*, Rev. Mod. Phys. **79** (2007), 519–553.

[22] Dietrich Küchemann, *Störungsbewegungen in einer gasströmung mit grenzschicht.*, Zeitschrift f. angew. Mathematik u. Mechanik. Bd 18, H. 4. Göttingen, Math.-naturwiss. Diss (1938).

[23] Sir Horace Lamb, *Hydrodynamics*, Dover Publications, Inc., 1945.

[24] L. D. Landau, *On the problem of turbulence*, Dokl. Akad. Nauk SSSR. **44** (1944), 339–343.

[25] L.D. Landau and E.M. Lifshitz, *Fluid mechanics, 2nd edition: Volume 6 course of theoretical physics*, Butterworth-Heinemann, 1987.

[26] J. F. McKenzie, *Reflection and amplification of acoustic-gravity waves at a density and velocity discontinuity*, J. Geophys. Res. **77** (1972), 2915–2926.

[27] A. Michalke, *On the inviscid instability of the hyperbolictangent velocity profile*, Journal of Fluid Mechanics **19** (1964), no. 4, 543–556.

[28] J. W. Miles, *On the reflection of sound at an interface of relative motion*, J. Acoust. Soc. Am. **29** (1957), 226–228.

[29] D. J. Needam and J. H. Merkin, *On roll waves down an open inclined channel*, Proceedings of The Royal Society A **394(1807)** (1984), 259–278.

[30] A. Paerhati and Y. Fukumoto, *An example exempted from thomsonctaitc-chetayev's theorem*, J. Phys. Soc. Jpn. **82** (2013).

[31] Suhas V. Patankar, *Numerical heat transfer and fluid flow*, Hemisphere Pub. Corp. ; McGraw-Hill Washington : New York, 1980 (English).

[32] Transmission Reflection and Amplification of Sound by a Moving Medium, *H. s. ribner*, J. Acoust. Soc. Am. **29** (1957), 259–279.

[33] Schiara M. Rosso, M. and J. Berlamont, *Flow stability and friction factor in rough channels*, J. Hydraulic Engineering, ASCE **116** (1990), 1109–1118.

[34] Takehiko Satomura, *An investigation of shear instability in a shallow water*, Journal of the Meteorological Society of Japan. Ser. II **59** (1981), 148–167.

[35] Helge Skovgaard, *Uniform asymptotic expansions of confluent hypergeometric functions and whittaker functions*, I Kommission hos J. Gjellerups Forlag, 1966.

[36] Naoki Takada, Junichi Matsumoto, and Sohei Matsumoto, *Phase-field model-based simulation of motions of a two-phase fluid on solid surface*, Journal of Computational Science and Technology **7** (2013), 322–337.

[37] S. Takehiro and Y. Hayashi, *Over-reflection and shear instability in a shallow-water model*, J . Fluid Mech. **236** (1992), 259–279.

[38] Geoffrey K. Vallis, *Atmospheric and oceanic fluid dynamics: Fundamentals and large-scale circulation*, Cambridge University Press, 2005.

[39] Sergio VASQUEZ, *A phase coupled method for solving multiphase problems on unstructured mesh*, ASME 200 Fluids Engineering Division Summer Meeting (2000).

[40] E W. Graham, *Effect of a shear layer on plane waves of sound in a fluid*, Journal of The Acoustical Society of America - J ACOUST SOC AMER **46** (1969).

[41] Jonathan M. Weiss, Joseph P. Maruszewski, and Wayne A. Smith, *Implicit solution of preconditioned navier-stokes equations using algebraic multigrid*, AIAA Journal **37** (1999), no. 1, 29–36.

[42] G. B. Whitham, *Linear and nonlinear waves*, Pure and Applied Mathematics, "A Willey-Intersience Series of Texts, Monographs, and Tracts", 1974.

[43] E. T. Whittaker and G. N. Watson, *A course of modern analysis*, 4 ed., Cambridge Mathematical Library, Cambridge University Press, 1996.

[44] P. A. Yakubenko and G. A. Shugai, *Over-reflection and instabilities in shear flows of shallow water with bottom friction*, Eur. J. Mech. B/Fluids **18** (1999), 931–957.

[45] Chia Shun Yih, *Stability of liquid flow down an inclined plane*, Physics of Fluids **6** (1963).